THE AGING CHARACTERISTICS OF A MEDIUM CARBON STEEL WITH
AND WITHOUT COPPER

A THESIS SUBMITTED TO
THE GRADUATE SCHOOL OF NATURAL AND APPLIED SCIENCES
OF
MIDDLE EAST TECHNICAL UNIVERSITY

BY

OSMAN EMRE UZER

IN PARTIAL FULFILLMENT OF THE REQUIREMENTS
FOR
THE DEGREE OF MASTER OF SCIENCE
IN
METALLURGICAL AND MATERIALS ENGINEERING

DECEMBER 2019

Approval of the thesis:

THE AGING CHARACTERISTICS OF A MEDIUM CARBON STEEL WITH AND WITHOUT COPPER

submitted by **OSMAN EMRE UZER** in partial fulfillment of the requirements for the degree of **Master of Science in Metallurgical and Materials Engineering Department, Middle East Technical University** by,

Prof. Dr. Halil Kalıpçılar
Dean, Graduate School of **Natural and Applied Sciences**   _____

Prof. Dr. C.Hakan Gür
Head of Department, **Met. and Mat. Eng.**   _____

Prof. Dr. Bilgehan Ögel
Supervisor, **Met. and Mat. Eng., METU**   _____

Assist. Prof. Dr. Kâzım Tur
Co-Supervisor, **...**   _____

Examining Committee Members:

Prof. Dr. Rıza Gürbüz
Met. and Mat. Eng., METU   _____

Prof. Dr. Bilgehan Ögel
Met. and Mat. Eng., METU   _____

Prof. Dr. Cevdet Kaynak
Met. and Mat. Eng., METU   _____

Prof. Dr. Abdullah Öztürk
Met. and Mat. Eng., METU   _____

Assist. Prof. Dr. Erkan Konca
Met. and Mat. Eng., Atılım University   _____

Date: 06.12.2019

I hereby declare that all information in this document has been obtained and presented in accordance with academic rules and ethical conduct. I also declare that, as required by these rules and conduct, I have fully cited and referenced all material and results that are not original to this work.

Name, Surname: Osman Emre Uzer

Signature:

ABSTRACT

**THE AGING CHARACTERISTICS OF A MEDIUM CARBON STEEL
WITH AND WITHOUT COPPER**

Uzer, Osman Emre
Master of Science, Metallurgical and Materials Engineering
Supervisor: Prof. Dr. Bilgehan Ögel
Co-Supervisor: Assist. Prof. Dr. Kâzım Tur

December 2019, 81 pages

For many years, copper bearing steels' usage in steel industry was limited by copper's detrimental effect on hot working capability. However with the latest findings that eliminates this negative effect with the addition of nickel, copper has emerged as an alloying element option. In various studies, copper is found to precipitate in ferrite phase after aging and leads to an increase in mechanical properties such as hardness and strength while still having a good amount of ductility-strength balance. In this thesis study, the effect of copper addition and the effect of copper precipitation hardening on medium-carbon steels which is not extensively studied previously will be addressed. To understand the effect, Cu-alloyed 4330M and 4330M medium carbon steels were cast and heat treated to obtain either martensitic or bainitic microstructure. These steels were then aged at various temperatures with different times and mechanical and microstructural properties of Cu-alloyed 4330M and Cu-free 4330M steels were compared. Copper was found to be retarding the softening in both martensitic and bainitic steels and Cu-alloyed bainitic steel yielded around 50 HV higher hardness values than that of 4330M when aged at 450°C for 270 minutes.

ÖZ

BAKIRLI VE BAKIRSIZ ORTA KARBONLU ÇELİKTE YAŞLANDIRMA ETKİLERİ

Uzer, Osman Emre
Yüksek Lisans, Metalurji ve Malzeme Mühendisliği
Tez Danışmanı: Prof. Dr. Bilgehan Ögel
Ortak Tez Danışmanı: Dr. Öğr. Üyesi Kâzım Tur

Aralık 2019, 81 sayfa

Bakır içeren çeliklerin, endüstriyel kullanımı geçmişte bakırın sıcak deformasyondaki olumsuz etkileri nedeniyle kısıtlanmış durumdaydı. Ancak bu konu üzerine yapılan çalışmalarda, bakırın bu olumsuz etkisinin alaşıma nikel ilavesi ile önlenebildiği görülmüş ve bakırın bir alaşım elementi olarak kullanılmasının yolu açılmıştır. Yapılan çalışmalarda, bakırın sertleştirme ısıl işleminden sonra ferrit içerisinde çökelerek, çelik mukavemet değerlerinde artışa neden olurken aynı zamanda süneklik-mukavemet dengesinde de iyi değerler gösteren çeliklerin üretilmesine olanak sağladığı gözlemlenmiştir. Bu tez çalışmasında daha önceki çalışmalarda ele alınmamış bir konu olan orta karbonlu çeliklerde bakır çökelmesinin etkilerinin ve bu çökelmenin mekanik özellikler üzerinde yapacağı etkilerin araştırılması amaçlanmaktadır. Etkinin anlaşılması için bakır içeren ve içermeyen 4330M kalitesine ait iki çelik alaşımı hazırlanarak dökümü yapılmış, sonrasında da beynitli ve martensitli yapı elde edilecek şekilde ısıl işlemlere tabi tutulmuştur. Daha sonra bu çelikler farklı süre ve sıcaklıklarda yaşlandırılarak, çeliklerin mekanik ve mikroyapı özellikleri karşılaştırılmıştır. Bakır içeren çeliğin yumuşatmayı geciktirici etkisi görülmüştür ve yine 450°C derecede 270 dakika yaşlandırılan bakır içeren beynitik

çeliğin sertlik değerinin bakır içermeyen çelikten 50 HV daha fazla olduğu görülmüştür.

Anahtar Kelimeler: Bakır, Beynit, Martensit, Yaşlandırma, Sementit Engellenmesi

To my beloved mother

ACKNOWLEDGEMENTS

TABLE OF CONTENTS

LIST OF TABLES

TABLES

LIST OF FIGURES

FIGURES

xvii

xviii

LIST OF ABBREVIATIONS

FCC: Face Centered Cubic

BCC: Body Centered Cubic

BCT: Body Centered Tetragonal

TTT: Time Temperature Transformation

Mf : Martensite Finish Temperature

Ms: Martensite Start Temperature

RA: Retained Austenite

M/A: Martensite/Austenite

ASTM: American Society for Testing and Materials

AISI: American Iron and Steel Institute

HV: Vickers Pyramid Number

RT: Room Temperature

CHAPTER 1

INTRODUCTION

Alloying and heat treatment process design have always been accepted as two of the best ways to improve mechanical properties of steel. Properties such as strength and ductility of martensitic and bainitic have been tried to be modified with different alloying additions and alternative heat treatment processes invented/evolved over the entire course of steel production history. Increasing the strength of the steel without compromising ductility and formability has been the major focus of studies.

Aging and tempering were two of the most preferred heat treatment processes to enhance mechanical properties of steel. These two processes are done at similar temperature intervals ranging from 100°C to 600°C. Tempering process is done to relieve stresses created during quenching of martensitic steel and it increases ductility of steel while accompanying some reductions in hardness and strength. Martensitic steels cannot be used as-quenched due to high degree of brittleness of quenched morphology and they are almost always tempered. On the other hand, aging is done to increase the strength of steel by precipitation hardening mechanism which is basically due to the dislocation-particle interaction [1]. It is the process of keeping steel at a temperature lower than austenization to enable to formation of fine precipitates that will act as obstacles to dislocation motion and cause strengthening [2]. The aging is applied later to austenitization which is followed by either quenching or bainitic transformation of steel after which the supersaturation of specific elements or compounds that will precipitate during aging are obtained. Aluminum, titanium, chromium, molybdenum and niobium are among the most common alloying elements used in steel for precipitation hardening [3]. Tempering and aging are co-existing procedures for martensitic steel since they are done at similar temperatures.

Copper, even if its usage has been limited in the past by hot shortness phenomena, can also be identified as one of the alloying element used for aging purposes. Copper precipitates are found to be formed in martensitic and bainitic steels in the shape of pure copper clusters after aging around 300°C to 600°C [4]. In many studies, it has been observed that these precipitates led to an increase in hardness and strength while not deteriorating the ductility and create a better strength-ductility balance. The use of copper in steel industry was previously restricted because of the hot shortness phenomena that is reduction in hot workability of steel due to the formation of low melting copper rich phase which lead formation of cracks at hot working temperatures. But this detrimental effect has been eliminated with alloying element additions such as nickel, manganese, boron and silicon. Nickel is found be most effective among those alloying elements as studies has shown [5].

In this thesis study, aging characteristics of Fe-Ni-Cu-X steel in martensitic and bainitic structures were investigated. Effect of copper addition on aging response of bainitic and martensitic structure and its effects on microstructural and mechanical properties are the focus point of the study. Contrary to the previous studies which mainly focused on ultra-low carbon or low carbon steels, present study addresses a medium-carbon steel. Cu-free and Cu-added versions of medium-carbon steel, 4330M, were produced with casting and fully bainitic and fully martensitic structure were tried to be obtained by quenching and isothermal transformations, respectively. The processing parameters are decided based on the steel compositions. Then steels were examined in terms of microstructure, hardness, strength, ductility and fracture behavior prior to and after aging heat treatment which provides a basis to understand the effect of copper precipitation.

The main goals of the study were to understand how copper addition affect aging characteristics of martensitic and bainitic steels and whether an increase in hardness and strength of steel or whether a retardation of softening is possible after aging/tempering for copper bearing steel in contrast with copper free steel as achieved in previous researches.

In addition to these, effects of heat treatment parameters such as aging time and temperature on the copper precipitation and on the mechanical properties of the steels were also investigated.

CHAPTER 2

LITERATURE REVIEW

2.1. Bainite

Bainite forms when austenitized steel is cooled with a higher rate than equilibrium during which transformation of pearlite is not possible and then isothermally treated above the martensite start temperature. On time-temperature-transformation (TTT) diagrams, bainite transformation temperature is between pearlite formation range in which diffusion-controlled transformation is possible and the martensite formation range in which diffusion is not possible. Bainitic steels can also be produced with continuous cooling instead of isothermal holding when bainite and pearlite formations are separated with alloying addition and when proper cooling rate is applied as shown on the Figure 2.1 below [6].
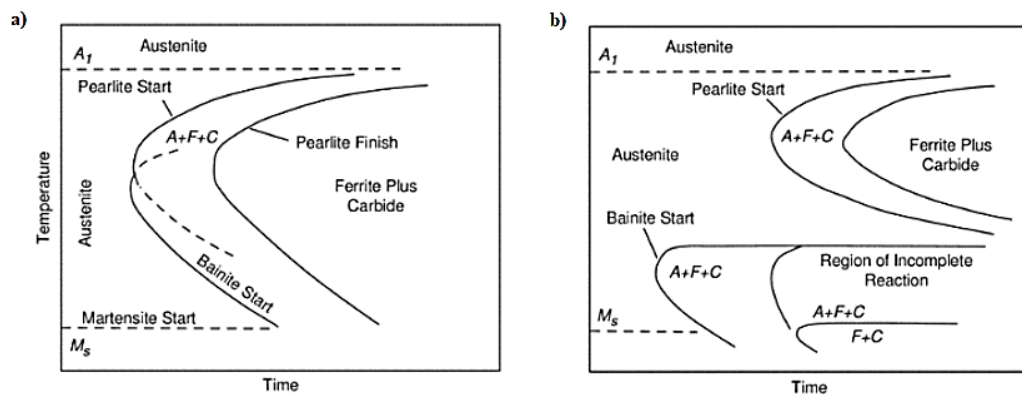
Figure 2.1. TTT diagram of a) plain carbon b) alloy steel [6]

Bainitic microstructure is similar to pearlitic microstructure put aside the fact that it's not lamellar. It is a combination of plate-like microstructure of ferrite and aggregates of non-lamellar cementite [7]. The ferrite plates are called sheaves and each sheave has its own sub-units. These sheaves have a wedge-shape and the thicker part of the

sheaf is near where nucleation begins. Each sub-units has to form from a carbon enriched austenite phase since during the formation of first sheave excess carbon partitions into neighbor austenite, as shown schematically in the Figure 2.2 below. Number 1, 2 and 3 show ferrite plates formed in enriched austenite [8].
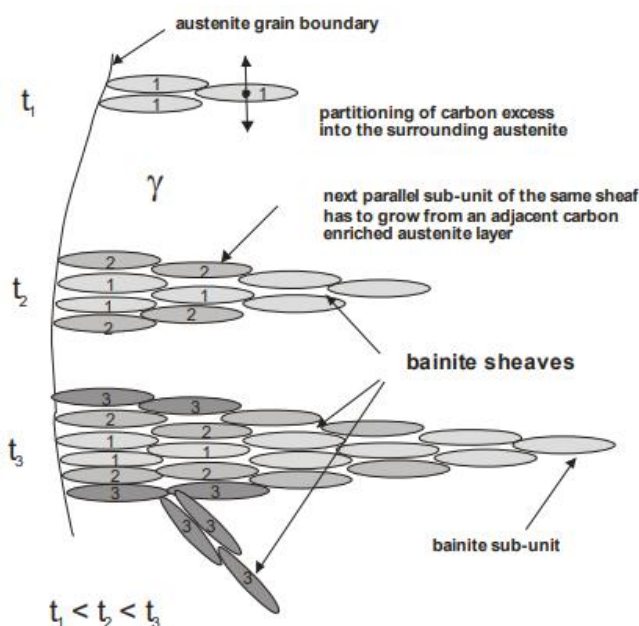
Figure 2.2. Formation of bainite sheaves at different times (t₁,t₂,t₃) [8]

The growth of these ferrite plates after nucleation is limited and these sheaves do not get thicker with prolonged isothermal holding. Since after transformation a shape change and strain are created and to relieve this strain, plastic deformation occurs in neighboring austenite phase. Dislocation density increases and impedes the growth of plates. The cementite found in bainite behaves differently based on transformation temperature and that's why the structure of bainite is dependent on transformation temperature [9]. There are two main types of bainite; upper and lower and the main difference between these two types is the existence of carbides in ferrite laths as shown in the next figure.

6
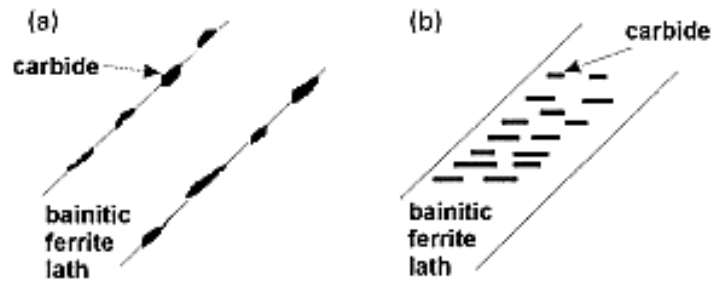
Figure 2.3. a) upper bainite b) lower bainite morphology [10]

2.1.1. Upper Bainite

In upper bainite, carbides precipitate from austenite between carbon enriched plates with the upper bainitic ferrite remaining free from carbides. Carbide precipitation starts when carbon content in austenite reaches a critical value during bainite reaction. To form upper bainite structure, the temperature must be in a range that the diffusivity of carbon is high enough to enable carbon transfer from newly formed ferrite to austenite. The temperature range is basically between 450 and 550°C [9].

The ferrite that forms during bainite formation has a fine lath structure. Cementite morphology resembles independent stringers in low carbon steels while in high carbon steels, stringer may become continuous.

2.1.2. Lower Bainite

In lower bainite, carbon precipitates from austenite like upper bainite while there is also a finer dispersion of plate-like carbides inside the ferrite plates. For carbon precipitate among ferrite plates, the temperature must be lower than upper bainite to trap the carbon inside ferrite plates and not to allow a high amount of diffusion into austenite. Transformation temperature is just above the martensite start temperature [11].

7

Figure 2.4. Formation of carbide precipitates inside of ferrite plates [9]

Morphology is similar to upper bainite with the existence of carbide precipitates in ferrite plates, as shown in Figure 2.4. Ferrite plates are much finer in lower bainite than upper bainite, which leads to higher number of orientations and high angle grain boundaries. This occurrence leads to higher strength in lower bainite. It has also much finer carbides than upper bainite and thus has higher toughness values. This can be explained by the fact that in lower bainite the cracks that are formed by finer carbides are smaller. These smaller cracks do not tend to propagate as much as larger cracks formed by coarser carbides [12][13].

2.1.3. Martensite/Austenite Constituent

One of the morphologies that can be formed during bainitic transformation is martensite/austenite constituent. It is a name given to a morphology consisting of untempered martensite found in carbon-rich retained austenite. During the bainitic reaction, a carbon enriched austenite phase is formed with a lower Ms than original concentration and if the bainitic transformation time is not enough to get fully bainitic steel, some of this retained austenite phase transforms into martensite. The ambient temperature must be lower than Ms of carbon enriched retained austenite [14]. This constituent is found as islands in microstructure and is called as M/A islands. An SEM image of this microstructure is shown in Figure 2.5.

8
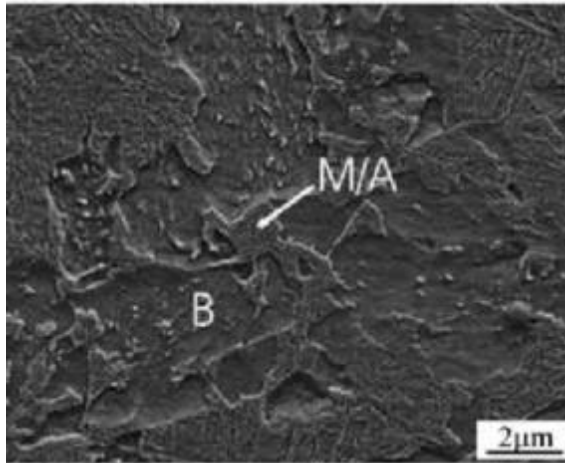
Figure 2.5. M/A island found in bainitic microstructure [15]

Bhadeshia has proposed that M/A found in steel can increase to resistance to crack propagation by transformation induced plasticity provided from austenite to martensite transformation during crack propagation. However, it is also stated that, if M/A islands become too coarse, they can create an embrittlement effect. For maximum resistance to crack propagation, these islands should be in the shape of films between lath and plates [9].

2.2. Martensite

Martensite in steel is formed as a metastable phase when steel is cooled down with a high cooling rate that will not allow diffusion of atoms. To form martensite, the cooling rate must be at a degree to avoid the nose of the TTT curve and this process is called quenching. Transformation occurs in a temperature range and to obtain fully martensitic structure, steel must be cooled rapidly below martensite finish temperature. Martensitic transformation is called diffusionless phase transformation and the main transformation mechanism is shear [16].

Due to the shearing mechanism, lattice distortion and thus high dislocation density are observed. This high dislocation density contributes to martensite being a strong phase. In addition to that, during fast cooling Face-Centered Cubic (FCC) austenite

transforms into Body-Centered Tetragonal structure (BCT) martensite and leads to volumetric expansion, which also adds to the strength of the martensite phase due to lattice distortion.

Martensitic structure can be summarized as needle-shaped plates or laths. There are two primary morphologies of martensite; strip and lamellar. Striped martensite forms at relatively higher temperatures above 200°C and has a structure of bundles of martensite. Lamellar martensite forms at lower temperatures below 200°C and has a large number of fine twins. It is also called as twin martensite. Morphology depends on carbon content and martensitic transformation temperature, which are interrelated. When martensitic transformation temperature is lowered, twin martensite is more likely to form while for high martensitic transformation temperature, the structure mainly consists of strip martensite as shown in the figure below [17].
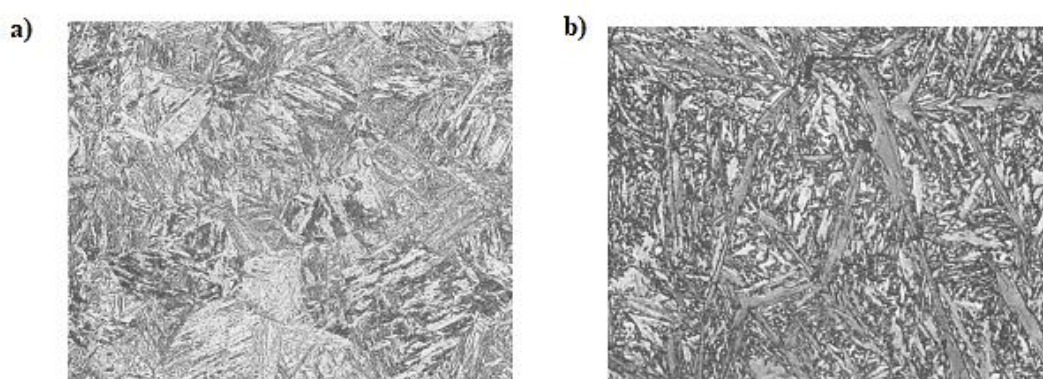
Figure 2.6. a) strip martensite b) lamellar martensite morphology [16]

Steel cannot be used in the form of as-quench microstructure because of the low toughness and ductility. Tempering is required for this type of steels which is basically reheating steel at a temperature lower than A1 temperature. Both yield and tensile strengths fall with the increasing tempering temperature but an increase in ductility and hardness is obtained [18]. Tempering helps to relieve of stress caused by volume expansion. Reactions during tempering occur in three stages. In stage 1, very small carbides are formed, a decrease in tetragonality of martensite is seen and low carbon

10

martensite is obtained. It is followed by a stage where retained austenite breaks into carbides and ferrite. In the last stage, small carbides formed in stage 1 are replaced with small particles of cementite, and low carbon martensite formed in stage 1 decomposes into ferrite [19][20].

2.3. Copper in Steels

To increase the recycling of steels, one of the most important topics is to get rid of the tramp elements. Copper, as one of these tramp elements, is tried to be utilized as an effective alloying element for steel instead of being gotten rid of. Studies have shown that it has the ability to strengthen steel through precipitation of fine copper particles when copper-containing steels are quenched from austenitic phase region which is followed by aging [21][22]. It was also studied that copper precipitation in iron might lead to achieving better strength-ductility balance than conventional high-strength steels because of a different nature of Cu precipitates from other precipitates like carbides and nitrides [23]. In addition to these, copper was found to be beneficial to corrosion resistance of steel [24].

Despite its all beneficial effects on steel properties, it is revealed that presence of copper could be detrimental to hot ductility of steel because of hot shortness phenomena which is one of the main reasons why copper has not been used as one of the main alloying elements in steel despite its positive effect on properties after aging. However, with the recent findings which will be mentioned in chapter 2.3.3 hot shortness phenomena caused by copper addition has been diminished.

Copper is also an austenite stabilizer that extends the formation of austenite over larger compositional and temperature ranges [25][26][27]. It decreases the eutectoid temperature of steel, which leads to a smaller inter-lamellar distance of pearlite due to low diffusion rate of carbon at lower temperatures. This situation leads to a rise in the hardness and strength of pearlitic steels [28].

Additionally, it acts as a suppressor for cementite precipitation similar to the effect of silicon. This can be explained with the fact that it's solubility in cementite is very low

and thus when the cementite is first formed and the mobility of atoms are slow due to low temperatures, copper becomes trapped inside it. This results in a decrease in the driving force of precipitation and precipitation kinetics are reduced [29][30].

2.3.1. Copper Precipitation Mechanism

To understand the strengthening mechanisms of copper in steel, its solubility and precipitation kinetics must be examined. The origin of precipitation of copper in steel is its low solubility in ferrite. The solubility of Cu in austenite is 2.3 % at 850 °C, while in ferrite, Cu exhibits a solubility of around 0.35 % at low temperatures. During the cooling of copper-bearing steel, extra copper that cannot be dissolved in ferrite forms precipitates. During aging, these precipitates follow a growing-transformation sequence. Studies have shown that precipitation begins with the formation of spherical clusters having a metastable BCC structure coherent with the ferrite matrix. When these clusters reach a critical size (characterized by a diameter of the order of 4 to 6nm), they transform to the equilibrium FCC structure and become incoherent. These incoherent precipitates are rod-like shaped, which is associated with minimizing strain energy. An intermediate 9R precipitate exists which has a size of 5 to 17 nm showing twinned FCC structure. The transformation from BCC to 9R is a martensitic type transformation [31]. Overall transformation sequence can be simplified as;

Solid solution - BCC - 9R – FCC [24]
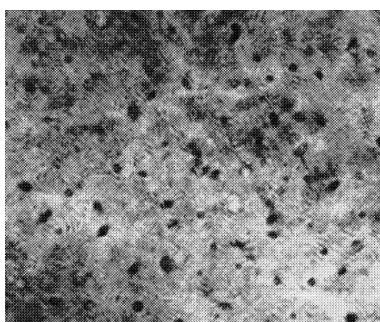
Figure 2.7. TEM micrographs of ferrite containing 1.5mass% Cu aged at 923 K for 1.8 ks showing copper precipitates as dark dots [32]

12

Despite the complex precipitation system, copper precipitation is selected because of their spherical geometry and being pure even at the early deformation stages. BCC precipitates are found to be the most effective type to increase the strength, which could be explained with its being coherent with the matrix [33].

Perez et al. [24] suggested the following formula for the solubility limit of copper in iron:

$$log[Cu]_{wt\%}^{GT} = \frac{5771323}{T^2} - \frac{15763.84}{T} + 9.944961$$

Also, with the data obtained from thermoelectric power measurements (TEP) a TTT diagram for precipitation of copper in iron could be drawn as shown in Figure 2.8. The use of these data could be useful to understand precipitation dynamics and also to determine heat treatment parameters.
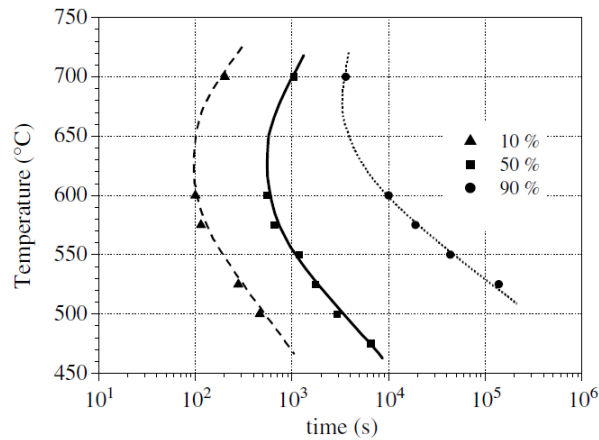
Figure 2.8. TTT diagram of precipitation reaction of copper [24]

In another study, copper precipitation in bainitic steel was studied, it was seen that both bainitic ferrite and cementite were copper saturated after isothermal bainitic transformation. To produce copper precipitates at ferrite and cementite, various aging temperatures were required. After aging treatments, Cu precipitates were seen as spheroidal and disperse particles with the size of 3-6 nm in both bainitic components

[7]. In a similar study on Fe-Cu bainitic steels, published by Foularis et al., it was observed that, elimination of copper supersaturation from ferrite was more downhill than in cementite during aging since the overcoming nucleation barrier was easier. The aging temperature used for eliminating copper supersaturation in ferrite was around 500°C, while it was possible for cementite around 550°C [9].

2.3.2. Effect of Copper on Steel Properties

When the studies on the effect of copper precipitation on steel properties are reviewed, it is seen that many studies support the fact that modification of steel with copper precipitates that are formed after aging provides higher strength, an excellent strength-ductility balance and higher corrosion resistance.

Takaki et al. [23] studied the effect of copper age hardening on low carbon ferritic and martensitic steels by adding 0, 1, 2 and 4 wt% Cu and compared their hardness after various aging times at different temperatures. Figure 2.9 shows the effects of aging temperature and time on maximum hardness difference between Cu free and 4 %Cu added ferritic steels. As it can be seen from this figure, a hardness increase around 140 HV can be seen for steel containing 4% Cu after aging at 500°C.
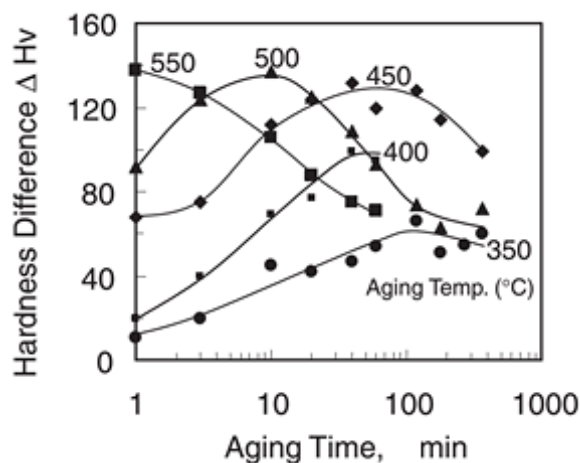
Figure 2.9. Effect of aging temperature and time on hardness difference between Cu free and 4 mass %Cu steel [23]

14

In the same research, the strength-ductility balance of copper containing steels is also investigated. Figure 2.10 shows tensile strength (TS) -elongation (El) plots for the tempered martensitic steels which is a good representation of this balance. A higher value of TS El, 20& greater than that of the Cu-free tempered martensite, was achieved for 4 wt %Cu steel with low aging temperature.
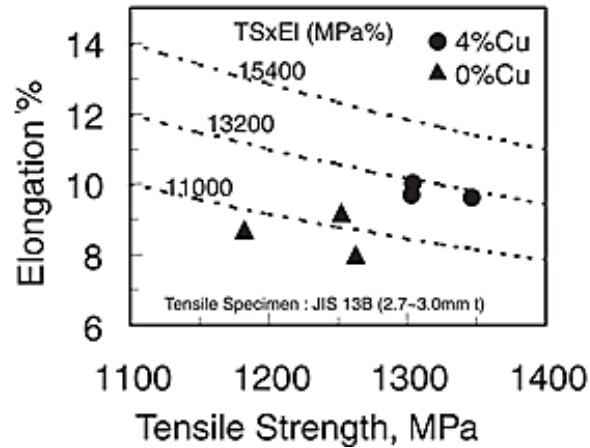
Figure 2.10. Tensile strength-elongation balance of Cu free and 4 mass%Cu steel [23]

Maruyama et al. [32] also studied a similar subject on ultra-low carbon steels which contains around 0.0013 wt% C. Copper free and 1.50 wt% copper added steels were compared in terms of hardness. It is found that a vast increase in hardness values of ferrite, deformed ferrite and martensite obtained after aging when 1.5% Cu is added as shown in Figure 5. The increase in hardness was around 180 HV for deformed ferrite 140 HV for ferrite and 40 HV for martensite.
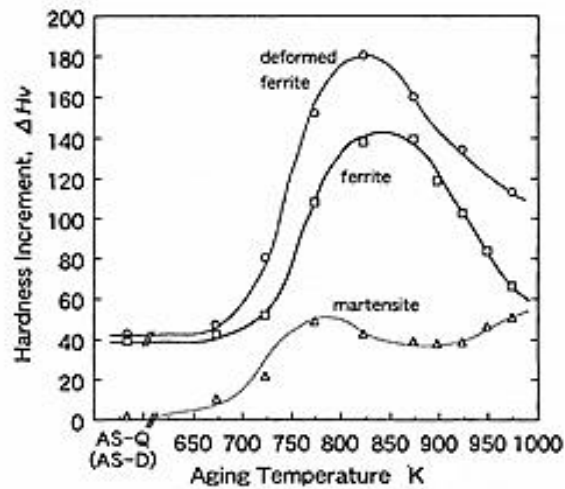
Figure 2.11. Hardness increment associated with copper addition in ferrite, martensite and deformed ferrite [32]

When the aging behavior of copper-bearing high strength low alloy steels is studied, by adding 1.98, 1.58, 1.23 wt% Cu to three different types of HSLA steels (S1, S2, S3) which are austenitized and water quenched, around 70 HV hardness increase was observed after aging for 2 hours at 450°C. The fall of hardness at aging times exceeding 2 hours was thought to be related with overaging.

The critical Cu precipitate size before overaging occurs was stated as 2.4 nm [34]. This critical precipitate size is also supported by another study as; the peak-aging by copper precipitate in iron is obtained when the precipitates are 2–3 nm [35].
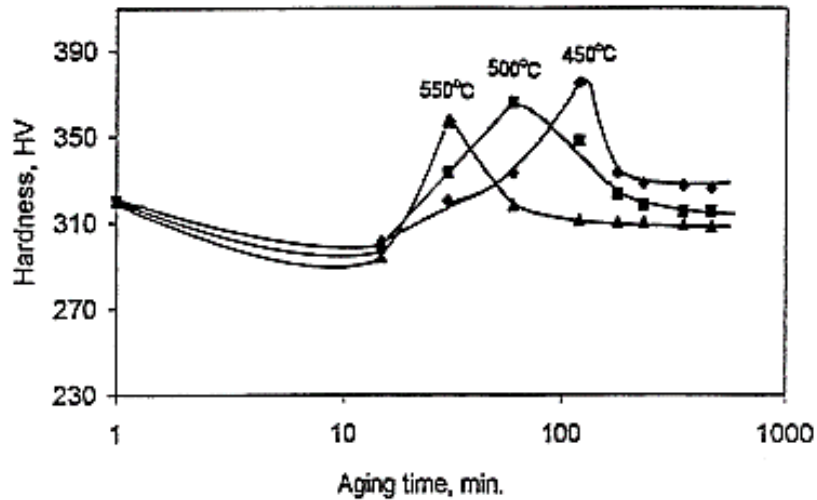
Figure 2.12. Change in hardness vs aging time for HSLA steel [34]

The hardness increase of martensitic and bainitic 1.08 wt % Cu bearing steels after aging were compared by Hsiao et al. and it was reported that bainitic steel responds in a better way. As it can be seen in the Figure 2.13, martensitic steel (cooled at 1°C/s) shows a decrease in hardness after tempering while bainitic steel (cooled at 120°C/s) shows an increase in hardness around 150 HV. This difference is explained by diminishing of carbon solid solution strengthening effect due to the precipitation of carbide particles during the initial stage of aging for martensitic steels. For bainitic structure, contrary to martensite, the existing carbide particles that become coarser carbides have little effect on strength. The softening effect of tempering is therefore always lower in bainite than in martensite. Therefore, the isothermal holding during aging treatment can highly contribute to the strength due to the precipitation hardening of copper-rich particles in bainitic steels [11].

17
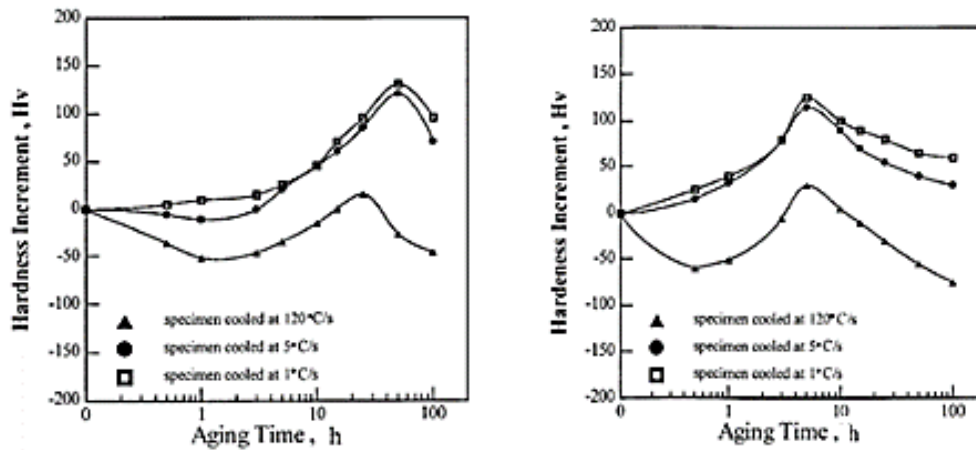
Figure 2.13. The aging response of 1.08 wt% Cu bearing steels after aging at 400°C and 500°C [11]

Some other studies have reported the following: an increase in tensile yield stress observed on aging of a binary Fe–1.67 atomic % Cu alloy quenched from 1000°C and aged to maximum yield stress at 475°C was 365 MPa [12]. In a low C steel containing 1.35% Cu, 0.8% Ni and 0.5% Mn, the increase in yield strength after aging from Cu precipitation was approximately 350 MPa [36].

Cu is also found to be increasing the strength of steel via solid solution hardening but compared to precipitation hardening, it is not a significant factor due to low solubility.

Another useful effect of copper addition in steel is to increase the corrosion resistance. Copper imparts weathering resistance in inland and marine environments and the high copper content in steel is effective in reducing the weight loss in weathering tests. Vaynman et al. [33] compared the corrosion losses of a number of plain carbon and weathering steels. Figure 2.14 shows that copper-bearing NUCu steel shows better weathering properties than ordinary weathering steels.

18
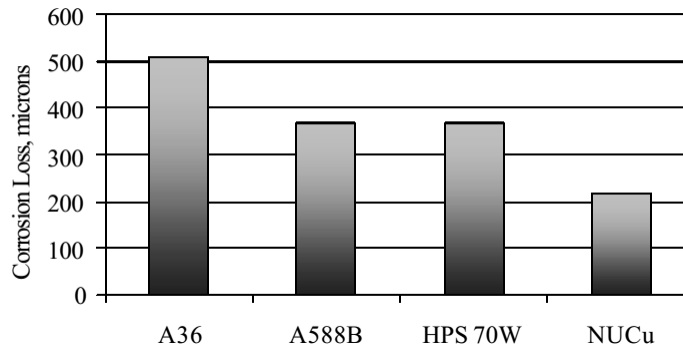
Figure 2.14. Results of the accelerated corrosion test (automotive SAE J2334 standard [33]

2.3.3. Hot Shortness

Despite all encouraging researches regarding the effects of copper precipitation on steel properties, copper-bearing steels still have limitations in production because of hot shortness phenomena. Hot-shortness occurs during the hot working of steel. Due to selective oxidation, Cu, Sn and other trace elements concentrate in the solid and the liquid state at the scale–metal interface. Penetration with grain-boundary diffusion along the grain boundaries weakens the cohesion of the grains and induces surface cracks during the hot working [37].
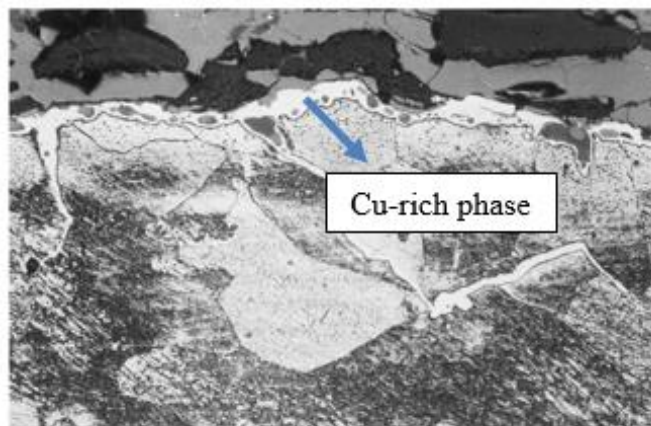
Figure 2.15. The concentration of Cu-rich phase below the scale after 4h of annealing at 1050°C [37]

Copper hot shortness simply works in the following steps. Firstly selective oxidation of iron occurs on the surface during reheating and leaves behind a Cu enriched phase.

19

Copper-rich phase becomes molten at temperatures above 1096°C [38]. Cu enriched phase goes into liquid form because of low melting point and diffuses along grain boundaries. Lastly, the molten phase weakens these boundaries and causes surface cracks during hot working.

Martinez et al. studied the effect of copper content on the crack index, the area of cracks found on the unit surface of AISI 1045 forging steel after deforming at 1130°C where selective oxidation of iron is possible. Results are shown in Figure 2.16, the crack index is found to be severely rising with increasing residual copper content in AISI 1045 steel [38].
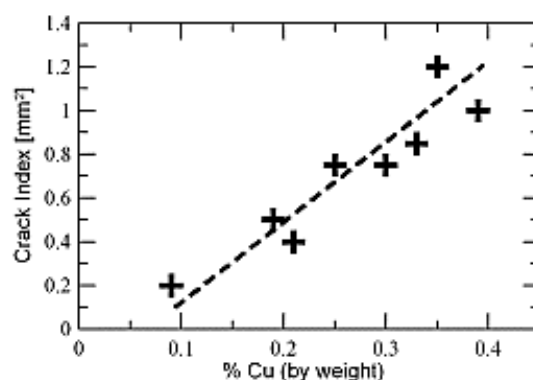
Figure 2.16. Crack index (mm^2) vs % Cu (by weight) [38]

To prevent the formation of hot shortness, it was established that the content of nickel should be half that of the copper content. Nickel increases the Cu-solubility in the austenite as well as favoring the occlusion of Cu in the scale. The effect of nickel results in the modification of the chemical composition of the phases, with a higher melting temperature, formed on the steel surface [5][37][39][40] that lower the tendency for hot cracks' formation. The beneficial effect of using the soaking temperature range of 1200–1300°C, with or without the presence of nickel, was also confirmed. The main reason for the absence of cracks in this high-temperature region is the rapid diffusion of the copper in the austenite. The diffusivity of copper in iron

is five times higher at 1200°C than at 1100°C. Result of this increased diffusivity is that despite the much higher oxidation rate at 1200°C than at 1100°C, the amount of copper-enriched phase at the steel–scale interface is smaller at 1200°C, compared with that at 1100°C. The occlusion of Cu rich phase is also accelerated with higher temperatures since the oxidation ratio and thickness of the scale are higher. However, due to these two parameters, the loss of material is also increased [39][41].

In another study by K. Shibata et al., other elements like Si, Mn, B and C were also found to be reducing susceptibility to hot shortness by either increasing occlusion of Cu by scale or restraining and reducing the penetration of liquid Cu phase into grain boundaries [42].

CHAPTER 3

EXPERIMENTAL PROCEDURE

3.1. Material

Table 3.1. *Chemical Composition of 4330M and Cu-alloyed 4330M Steels*

Steel	C	Si	Mn	Cr	Mo	Ni	Al	Cu	Ti	V
4330M	0.29	0.42	0.97	0.73	0.41	1.30	0.015	0.05	0.001	0.02
Cu-alloyed 4330M	0.29	0.41	0.94	0.72	0.39	1.29	0.006	1.95	0.001	0.02

To understand the effect of copper on the steel, two different compositions of casting alloy were designed; one is Cu free and the other is Cu added. Alloy preparation in commercial size induction furnace and the casting of the liquid steel alloys into modified Y-block molds were done at Anadolu Döküm A.Ş-Körfez-Kocaeli.

AISI 4330 (4330M) modified grade steel was chosen as the reference steel because it contains nickel, which is effective in eliminating the hot shortness effect of copper addition. 4330M steel has higher chromium, nickel and vanadium content than that of regular 4330.

The compositions of the prepared alloys were analyzed with ARL 4460 Optical Emission Spectrometer at Anadolu Döküm Quality Laboratories and given with Table 3.1.

Both 4330M and Cu-alloyed 4330M steel were cast into the same Y-block type sand molds. There were simply two sections of the mold design; riser and sound casting section. The sound casting section is in the shape of two rectangular bars of 35x30x270 mm for both 4330M and Cu-alloyed 4330M steel casting. The riser section of the

casting is not used for the mechanical tests as it contains high amount of shrinkage porosity. However it would be suitable for initial heat treatments and subsequent microstructural examinations.

Figure 3.1. The figure of cast of (2) 4330M (6) Cu-alloyed 4330M steels (During pouring into molds, risers were on top. The photo taken after the risers and the casting were separated by cutting)

3.2. Testing Procedure

The testing procedure follows the route described in Figure 3.2. Sampling for metallographic examinations and mechanical tests was done at three stages as shown in Figure 3.3.

1. Prior to austenitizing to understand as-cast properties
2. After oil quenching (martensitic transformation) and, after isothermal hold in salt bath (bainitic transformation)
3. After aging/tempering process

24
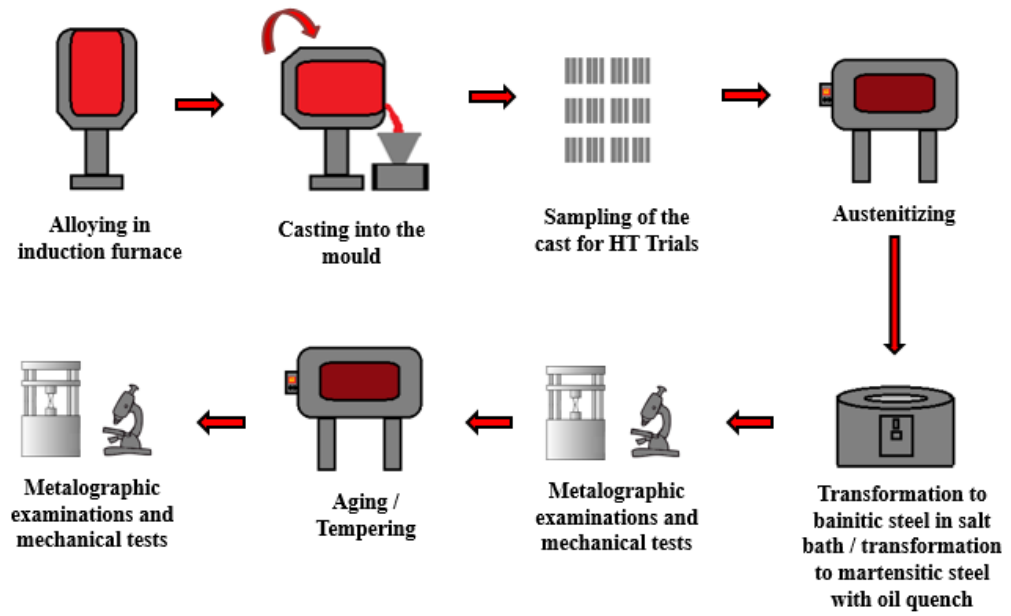
Figure 3.2. Testing Procedure and Sampling Scheme
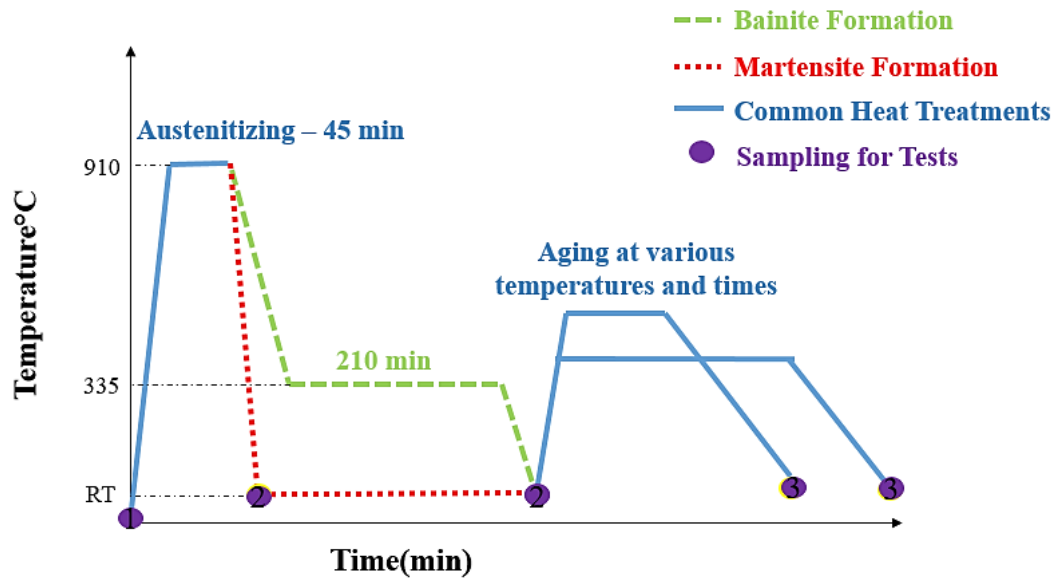
Figure 3.3. Sampling Stages

3.2.1. Heat Treatment Procedure

3.2.1.1. Heat Treatment Equipment

For austenitization and tempering/aging procedures, Protherm muffle furnace was used. Protherm PC442T thermocouple was used for temperature measurements. For quenching, oil is used for quenching media. A salt bath with a capacity of 8.5 L, containing AS 135 Tempering Salt which is a nitrate-nitrite mixture, is used for keeping steel isothermally at different temperatures. The working range of the salt in the bath is 160°C-550°C.

3.2.1.2. Heat Treatment Parameters

For the determination of heat treatment parameters, JMatPro the Materials Property Simulation Package Version 6.1 was used.
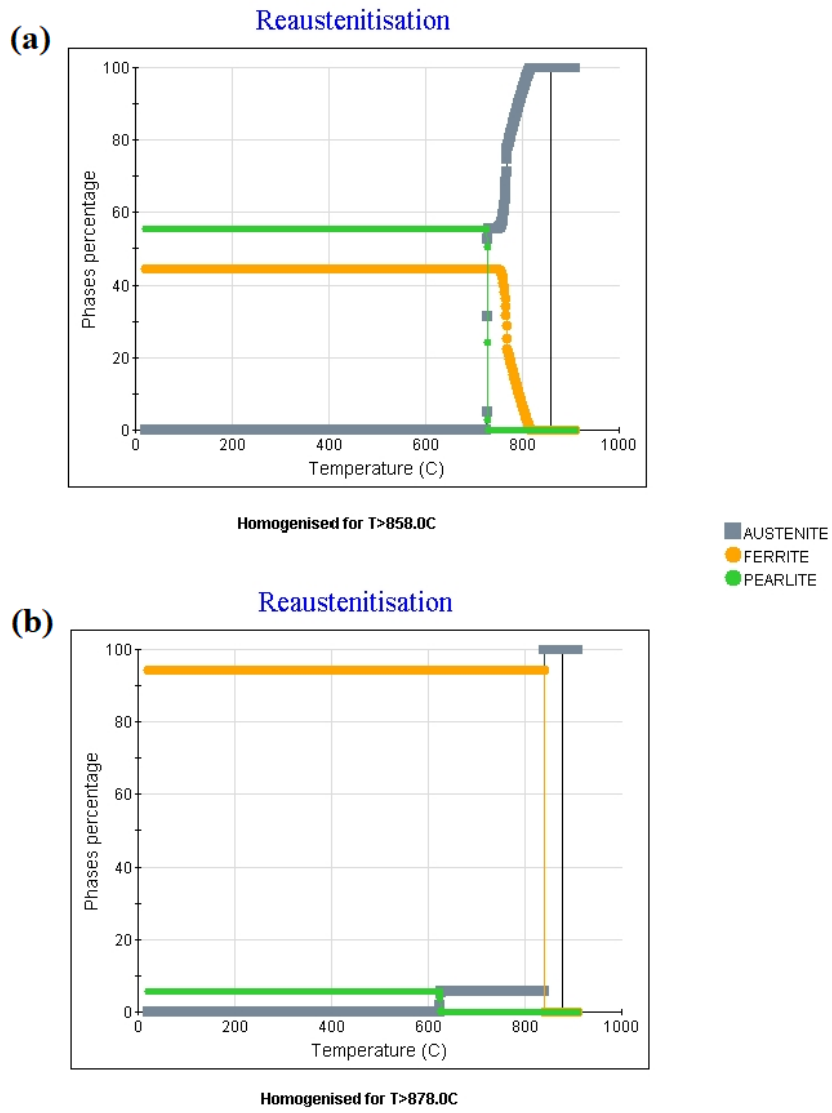
Figure 3.4. Reaustenization temperatures of a) 4330M b) Cu-alloyed 4330M steels constructed by JMatPro

27

COMPOSITION (Wt%)
Fe: 93.8926
Al: 0.0056
Cr: 0.724
Cu: 1.95
Co: 0.0124
Mn: 0.938
Mo: 0.394
Nb: 0.0083
Ni: 1.29
Si: 0.41
Ti: 0.0010
V: 0.0169
W: 0.0080
B: 0.0085
C: 0.287
N: 0.0121
P: 0.0327
S: 0.0089
TRANSITIONS: (C)
Pearlite: 709.9
Bainite: 539.5
Ferrite: 747.0
Martensite:
  Start: 313.0
  50%: 277.2
  90%: 194.1

Grain size : 100 microns
Austenitisation : 910.0 C
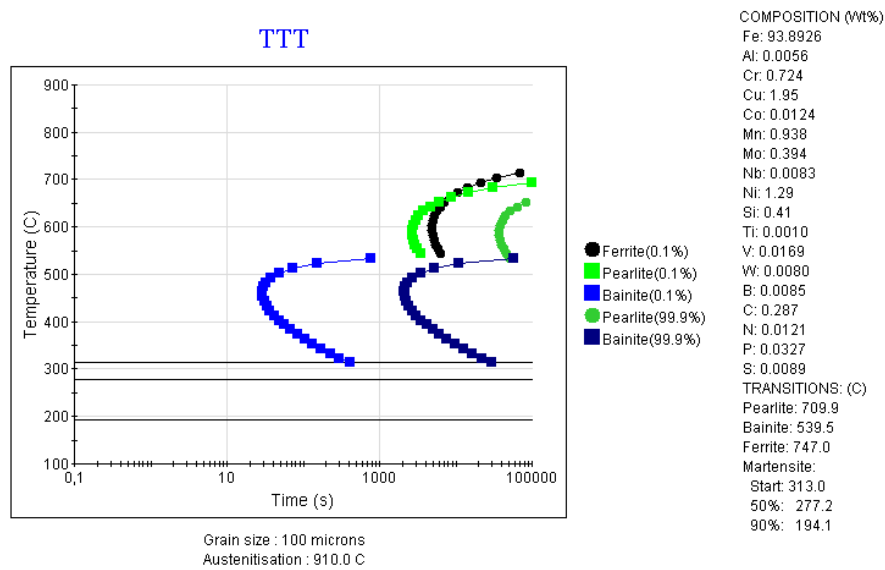
Figure 3.5. TTT diagram of Cu-alloyed 4330M steel constructed by JMatPro

COMPOSITION (Wt%)
Fe: 95.735
Al: 0.0145
Cr: 0.733
Cu: 0.0475
Co: 0.012
Mn: 0.965
Mo: 0.407
Nb: 0.0088
Ni: 1.3
Si: 0.415
Ti: 0.0010
V: 0.0151
W: 0.0080
B: 0.0085
C: 0.294
N: 0.0165
P: 0.0191
TRANSITIONS: (C)
Pearlite: 720.8
Bainite: 535.6
Ferrite: 772.8
Martensite:
  Start: 327.0
  50%: 291.6
  90%: 209.5

Grain size : 100 microns
Austenitisation : 910.0 C
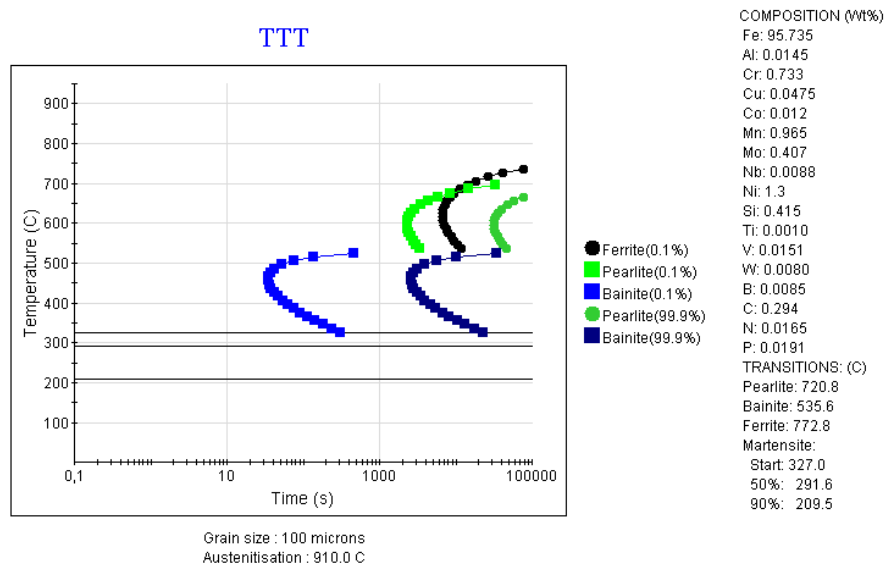
Figure 3.6. TTT diagram of 4330M steel constructed by JMatPro

20x20x80 mm rectangular sections were cut from the 4330M and Cu-alloyed 4330M castings to be heat treated. Austenization temperature was selected to be 910°C, whereas suggested temperatures by JMatPRo were 878°C for Cu-alloyed 4330M and 858°C for 4330M steel as shown with Figure 3.4. Austenization time was fixed to be

45 minutes. For bainitic transformation temperature and time in which steel will be kept isothermally, 335°C and 3.5 hours are selected considering the suggested data by JmatPro as shown in Figures 3.5 and 3.6. After salt bath holding, the samples were still air cooled. Oil is used as quench media for the production of martensitic microstructure. After bainitic and martensitic steels are obtained, these samples were cut into smaller, approximately 10x10x10 mm cubes for subsequent tempering/aging at various temperatures and times. These are then used for microstructural examinations and hardness measurements.

3.2.2. Microstructural Examinations

Microstructural examinations were done by using optical microscopy and SEM. To prepare specimens for the examinations, Metkon Metacut 251 Abrasive Cutter was used as cutter. For the samples that have been heat-treated, at least 2 mm is removed from the surface to remove the decarburized layer. Metkon Ecopress 100 was then used to mount the specimens into bakelite. Samples were grinded using Metkon Gripo 2V Grinder and Polisher. Samples were polished by Mecapol P230 Polisher using 6μm and 1μmMetkon Diapat-P water-based diamond solutions.

Specimens were etched with 2% Nital solution for 15 to 20 seconds prior to examinations.

Optical microscopy was done using Huvitz Digital Microscope HDS-5800 and Nikon Optiphot 100. Electron metallographic examinations were performed using FEI 430 Nano Scanning Electron Microscope. The same SEM is also used for the examinations of fracture surfaces of tensile test specimens.

For the calculation of phase fractions of microstructure, ImageJ image analyzing software was used.

3.2.3. Hardness Measurements

For hardness measurements, Emco Universal Digital Hardness Testing Machine's Vickers indenter and the load of 30kgf were used. For every sample, the measurements were repeated at least 3 times.

3.2.4. Tensile Test

INSTRON 5582 Universal Tensile Test Machine was used for the tensile test. For each different heat treatment condition, 2 tensile specimens were tested due to the limited specimen availability. Tensile test specimens were machined according to ASTM E8/16a standard M12.

Tensile strain data was collected by an optical extensometer, which measures the distance between two dots placed on tensile specimen gage before the test.
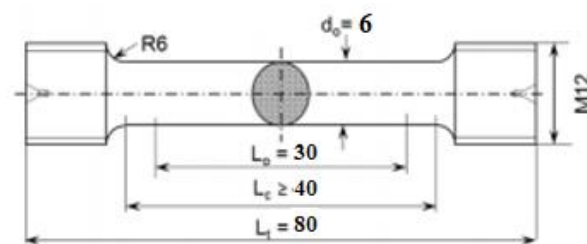
Figure 3.7. Dimensions of tensile test specimen, all in mm [43]

CHAPTER 4

EXPERIMENTAL RESULTS

4.1. Simulation Results of TTT Diagrams

JMat Pro is used to determine heat treatment parameters to produce bainitic and martensitic microstructures.
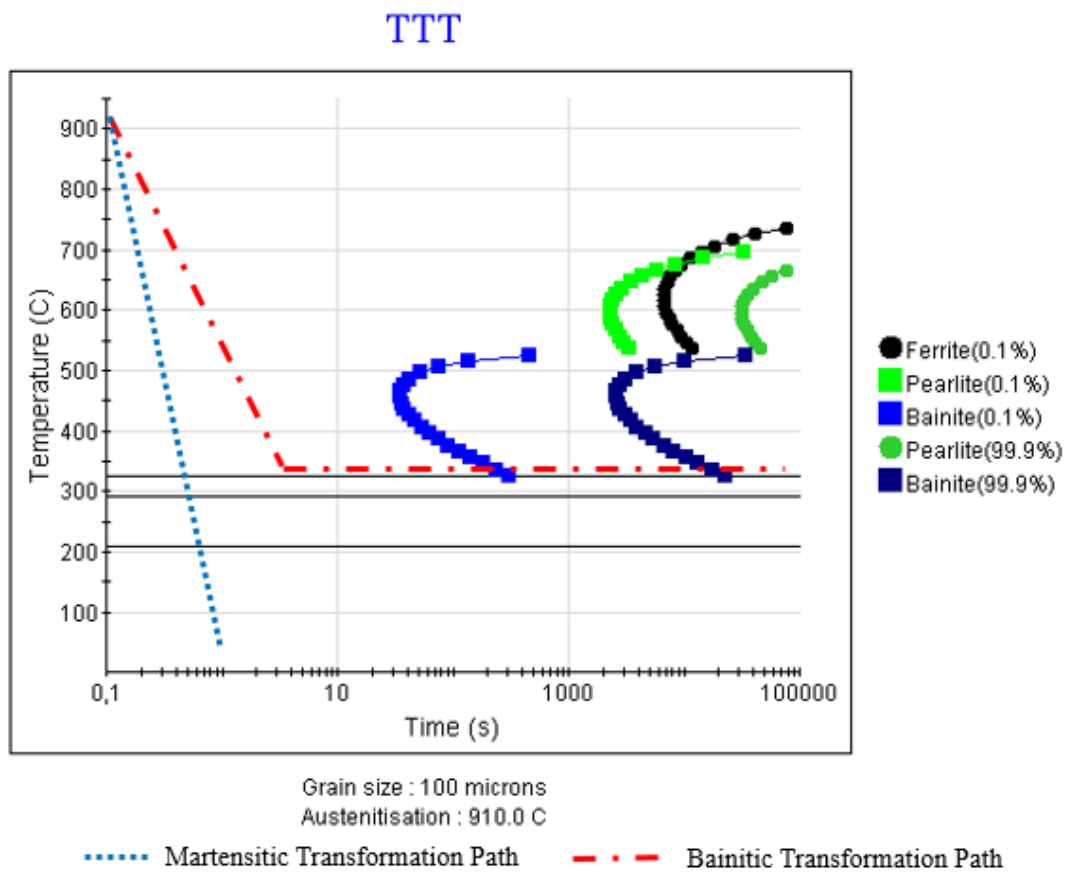
Figure 4.1. Transformation paths of 4330M steel on TTT diagram
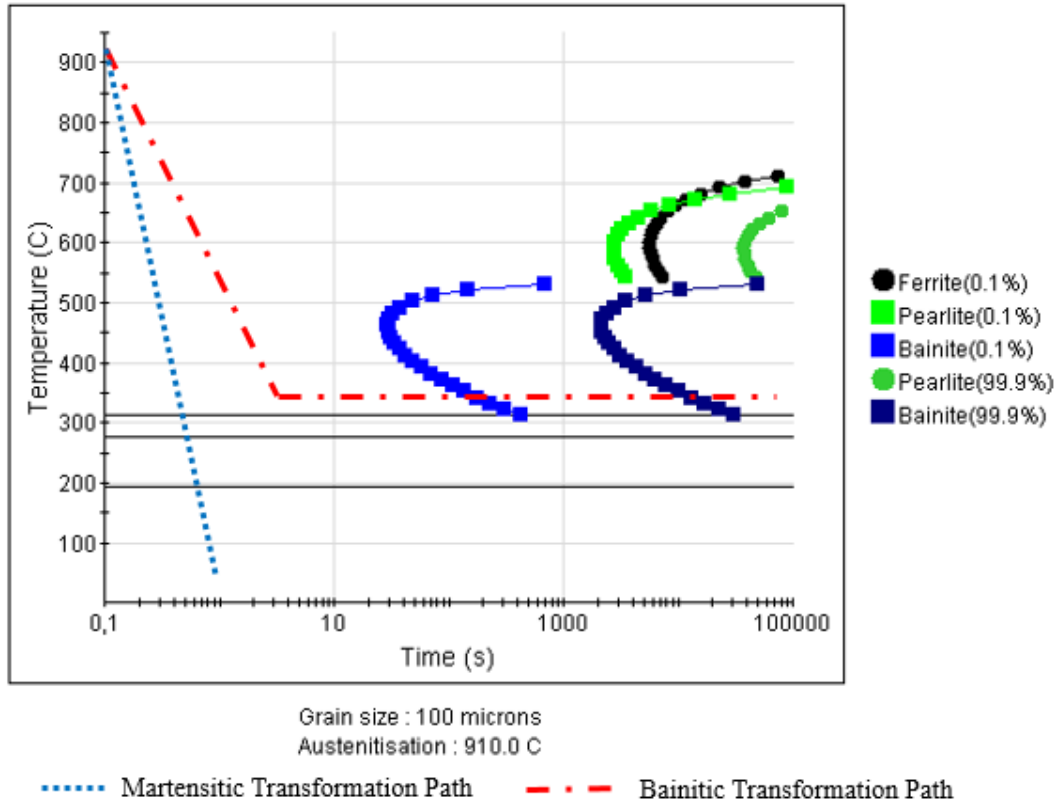
Figure 4.2. Transformation paths of Cu-alloyed 4330M steel on TTT diagram

From the JMat data, austenization temperature is suggested to be 878°C for Cu-alloyed 4330M and 858°C for 4330M as stated previously; however the temperature was selected as 910°C to stay on the safe side.

M_s for Cu-alloyed 4330M was predicted to be 313°C while it is 327°C for 4330M.

Fully bainitic transformation time is predicted to be 211 and 198 minutes for Cu-alloyed 4330M and 4330M, respectively.

To heat treat the samples in the same batch, the bainitic transformation parameters were selected to be the same for both steel alloys. Isothermal transformation was carried out at 335°C for 210 minutes which should be enough to obtain fully bainitic structure for both steel according to JMatPro data. Heat treatment parameters predicted by JMatPRo are summarized in Table 4.1.

To produce martensitic structure, all specimens were austenitized at 910°C for 45 minutes then quenched in oil. For the remaining parts of this thesis samples that have been put through this treatment will be named as martensitic steels.

To produce bainitic structure, all specimens were also austenitized at 910°C for 45 minutes, then isothermally treated at 335°C for 3.5 hours. For the remaining parts of this thesis samples that have been put through this treatment will be named as bainitic steels

Table 4.1. *Transformation temperature and times found from TTT diagrams constructed by JMat*

Type of Steel	Type of Transformation	Transformation Temperature (°C)	Transformation Time (min)
4330M	M_s	327	-
	M_f	210	-
	0% Bainite	327	5
	100% Bainite	327	216
Cu-alloyed 4330M	M_s	313	-
	M_f	194	-
	0% Bainite	313	2
	100% Bainite	313	200

4.2. Microstructural Examinations

4.2.1. Microstructural Examinations of As-Cast Steels

Figure 4.3. The as-cast microstructure of 4330M under optical microscopy

Figure 4.4. The as-cast microstructures of Cu-alloyed 4330M under optical microscopy

34

As-cast microstructures of both steel alloys were examined to understand the effect of Cu on as-cast microstructure and the results are shown in Figures 4.3 and 4.4. Characterization of the as-cast microstructures cannot be made clearly because of the dendritic solidification characteristics of casting.

Dendritic structure of as-cast steel is also shown in Figure 4.5.

Figure 4.5. Dendrites observed in as-cast Cu-alloyed 4330M microstructure at a lower magnification.

SEM micrographs of as-cast steels are shown in Figure 4.6 and 4.7. Pearlite as lamellar structure and pro-eutectoid ferrite as dark phase can be identified.
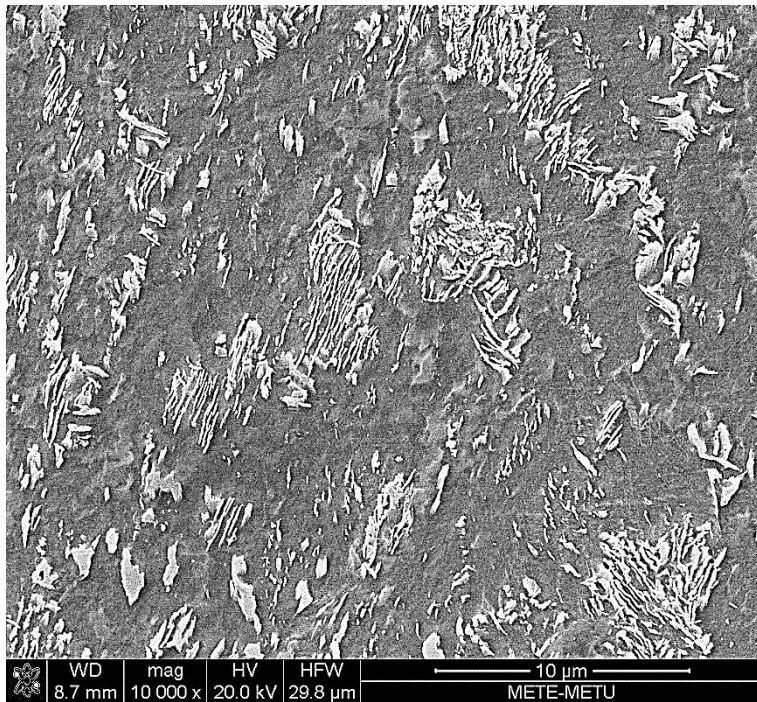
Figure 4.6. SEM micrographs of as-cast 4330M
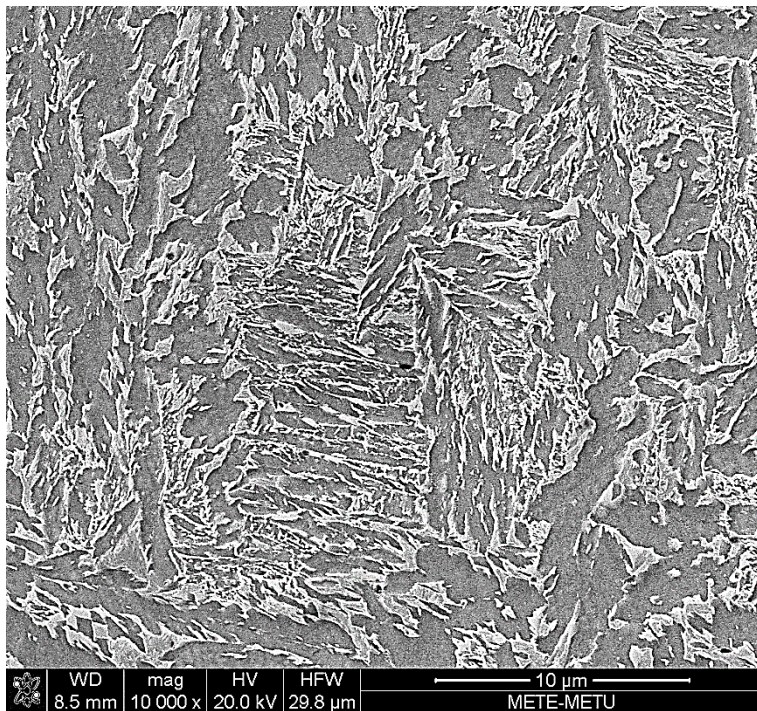
Figure 4.7. SEM micrographs of as-cast Cu-alloyed 4330M

Table 4.2. *Phase Fractions of As-Cast Steel Found by ImageJ Application*

Type of Steel	SEM Image(5000X)	Constructed Phase Fraction Image by ImageJ	Phase Fractions
4330M			25.6%White 74.4%Gray
Cu- Alloyed 4330M			36.6%White 63.4%Gray
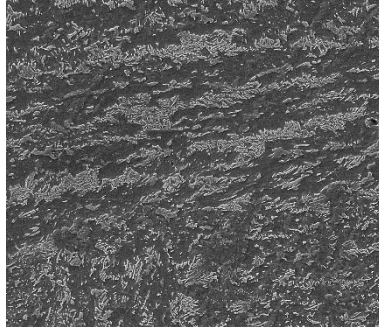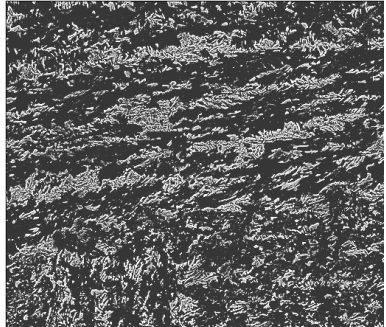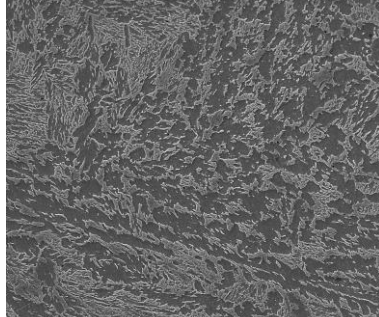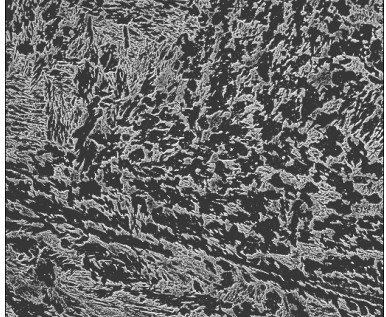
With the use of ImageJ image analyzing software, pearlite is colored with white while the matrix is gray. The fraction of pearlite is found to be 25.6% and 36.6% for 4330M and Cu-alloyed 4330M, respectively. These are shown in Table 4.2.

4.2.2. Microstructural Examinations of Martensitic Steels

4.2.2.1. Quenched Microstructures
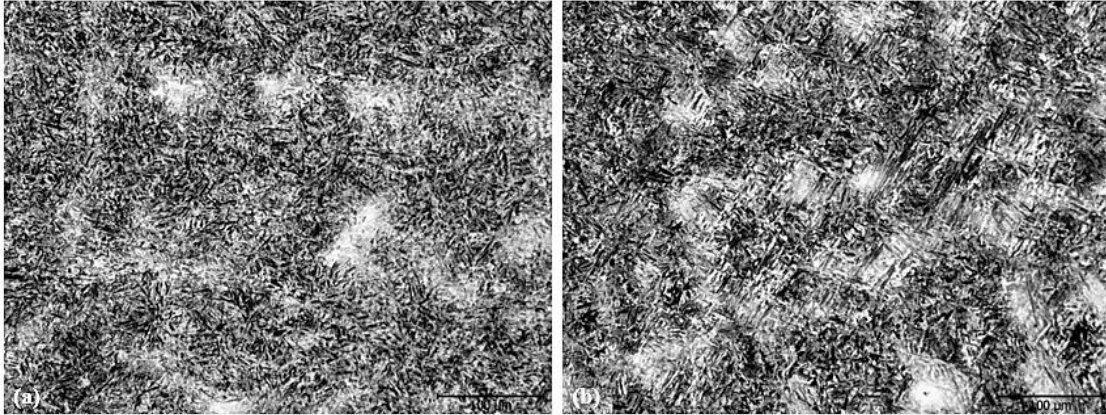
Figure 4.8. . (a) 4330M and (b) Cu-alloyed 4330M martensitic steels under optical microscope at low magnification
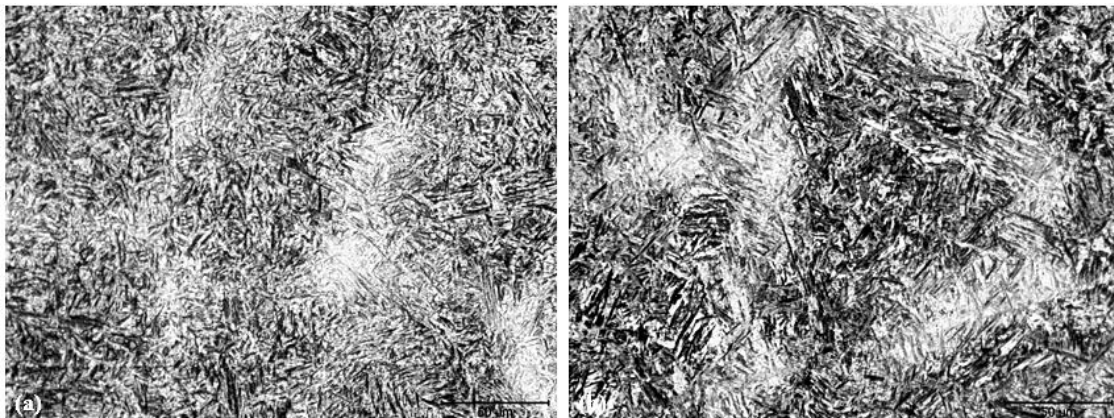
Figure 4.9. (a) 4330M and (b) Cu-alloyed 4330M martensitic steels under optical microscope at high magnification

With the optical metallography of Cu-alloyed 4330M and 4330M steels were austenitized at 910°C for 45 minutes followed by oil quenching, fully martensitic structure is clearly seen for both steels as shown in Figure 4.8 and Figure 4.9.
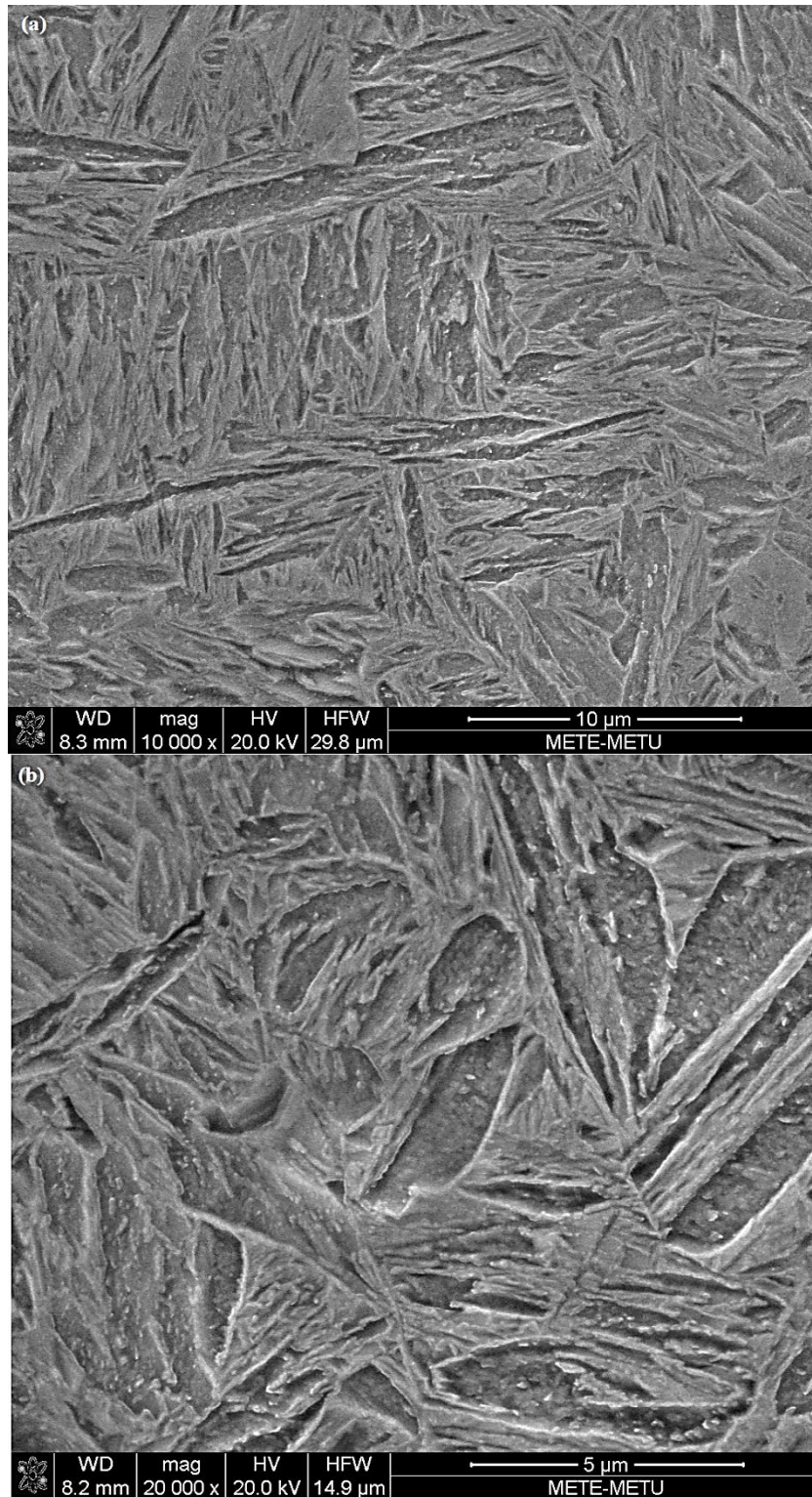
Figure 4.10. SEM micrographs of martensitic 4330M obtained (a) at low magnification, (b) at high magnification
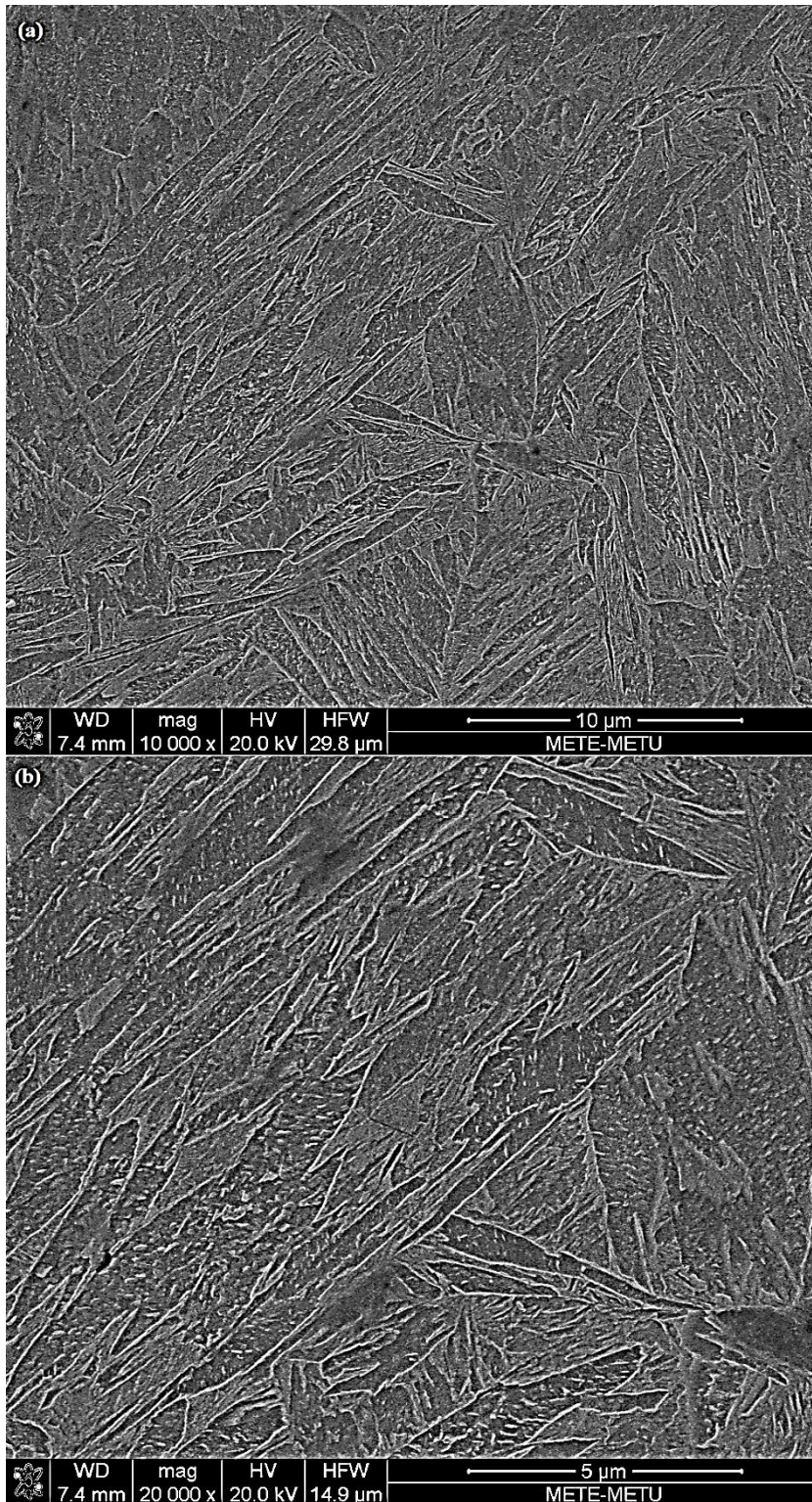
Figure 4.11. SEM micrographs of martensitic Cu-alloyed 4330M (a) at low magnification, (b) at high magnification

SEM micrographs shown in Figures 4.10 and 4.11 are parallel to optical micrographs. Random distribution of martensite laths are observed for both Cu-free and Cu-added steel.

4.2.2.2. Quenched and Tempered/Aged Microstructures

Microstructures of 4330M and Cu-alloyed 4330M martensitic steels after aging are also examined. Figure 4.12 and 4.13 shows SEM micrographs for steel samples after aging at 500°C for 90 minutes.

Tempered martensite microstructures were observed for both steel with no significant difference in martensitic morphology as expected.
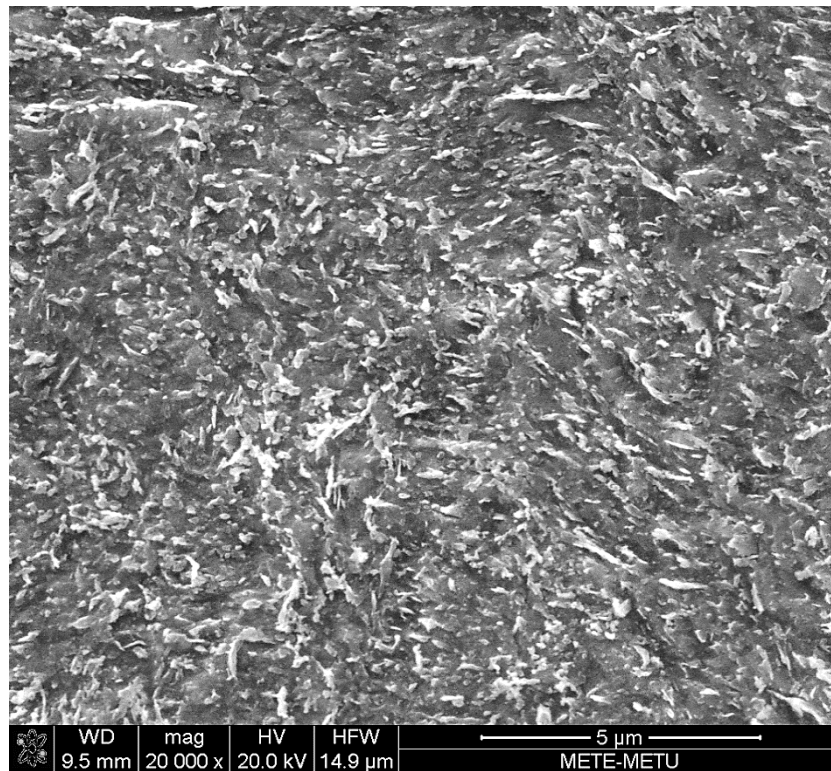
Figure 4.12. SEM micrograph of martensitic 4330M aged at 500°C for 90 minutes
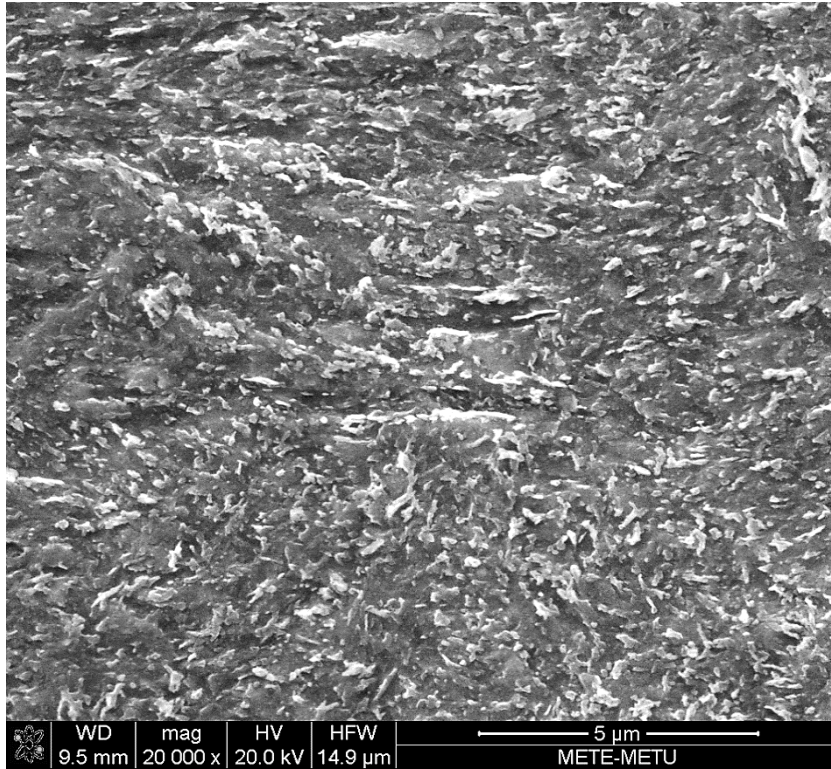
Figure 4.13. SEM micrograph of martensitic Cu-alloyed 4330M aged at 500°C for 90 minutes

4.2.3. Microstructural Examinations of Bainitic Steels

4.2.3.1. Isothermally Transformed Microstructures

Figures 4.14 and Figure 4.15 show optical micrographs of 4330M and Cu-alloyed 4330M steels, which are austenitized at 910°C for 45 minutes and then isothermally treated in a salt bath at 335°C for 210 minutes. Both types of steels have gone through bainitic transformation and primarily consisting of mixture of bainite which is the dark phase and M/A islands, the bright phase. However, the population of M/A islands is much higher in Cu-alloyed 4330M as seen from Figure 4.14 a and b.
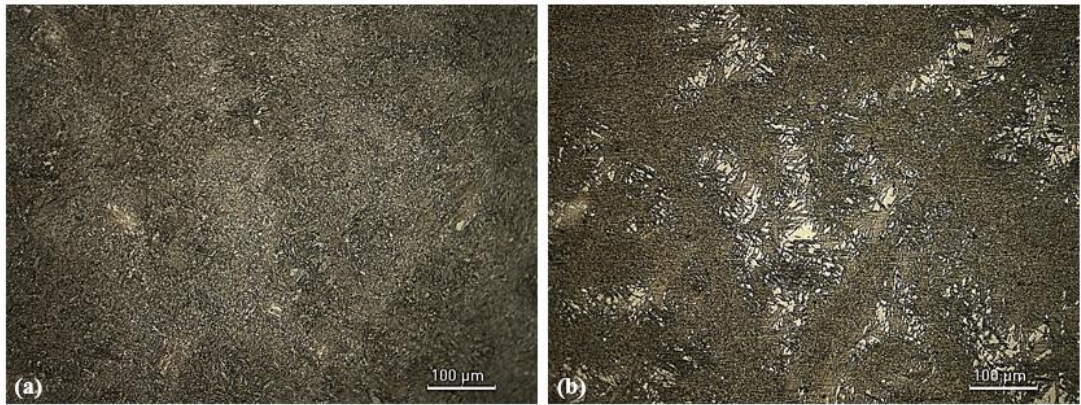
Figure 4.14. (a) 4330M and (b) Cu-alloyed 4330M bainitic steels under an optical microscope at a low magnification
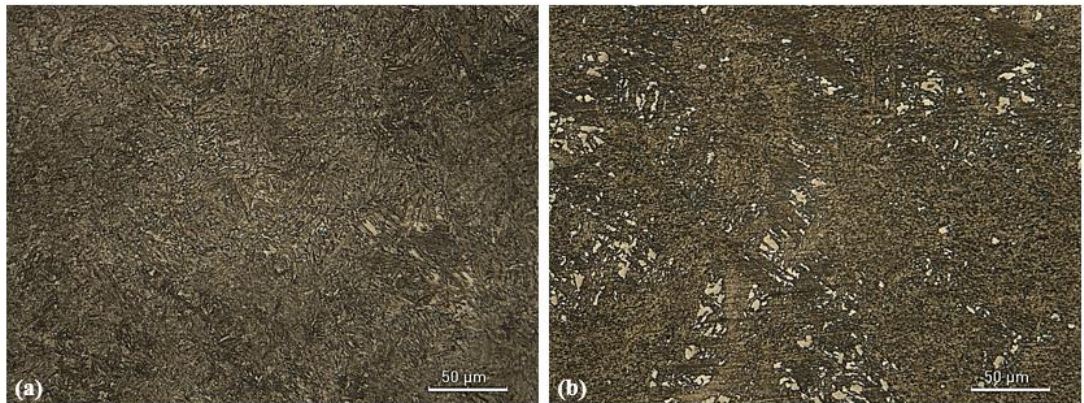
Figure 4.15. (a) 4330M and (b) Cu-alloyed 4330M bainitic steels under an optical microscope at a high magnification

Table 4.3. *Phase Fractions of Bainitic Steel Found by ImageJ Application*

Type of Steel	Optical Image	Constructed Phase Fraction Image by ImageJ	Phase Fractions
4330M			2.5% White 97.5% Gray
Cu-alloyed 4330M			13.0% White 87.0% Gray
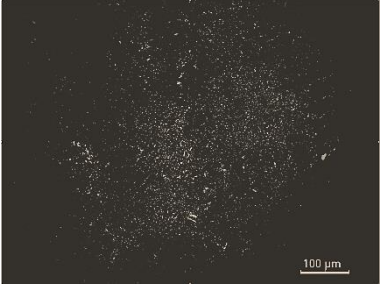
With the help of ImageJ image analyzing software, M/A islands are colored with white while the matrix is gray. The fraction of M/A islands is found to be 2.5% and 13% for 4330M and Cu-alloyed 4330M, respectively. These are shown in Table 4.3
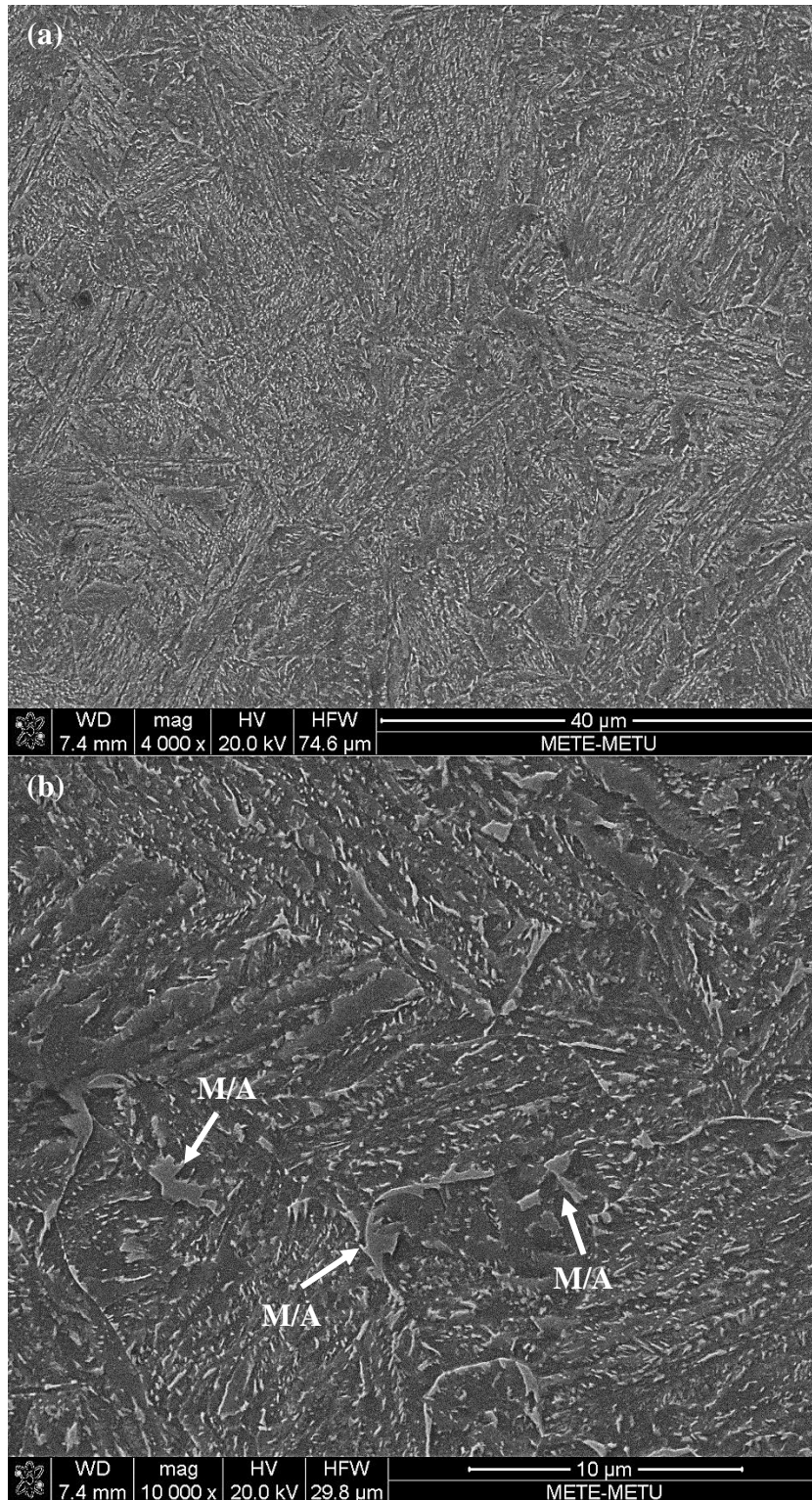
Figure 4.16. SEM micrographs of bainitic 4330M (a) at low magnification, (b) at high magnification, showing M/A constituents and bainitic matrix with carbide precipitation
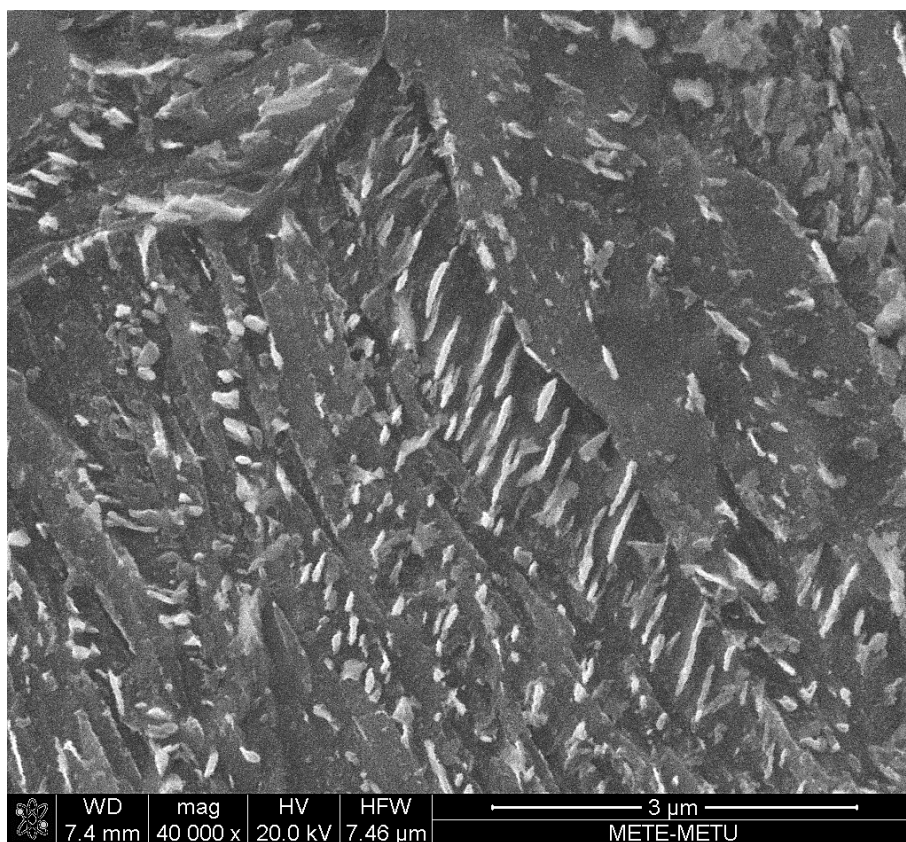
Figure 4.17. SEM image showing carbide precipitation in bainitic matrix of 4330M

SEM examination of bainitic 4330M has also shown that the microstructure is a mixture of M/A island and bainite sheaves. M/A islands could not be detected at low magnification but can be observed at high magnifications as shown in Figure 4.16-b.

Carbide precipitation in bainite is also observed and small rod-shaped carbides within bainite sheaves are observed as shown in Figure 4.17.
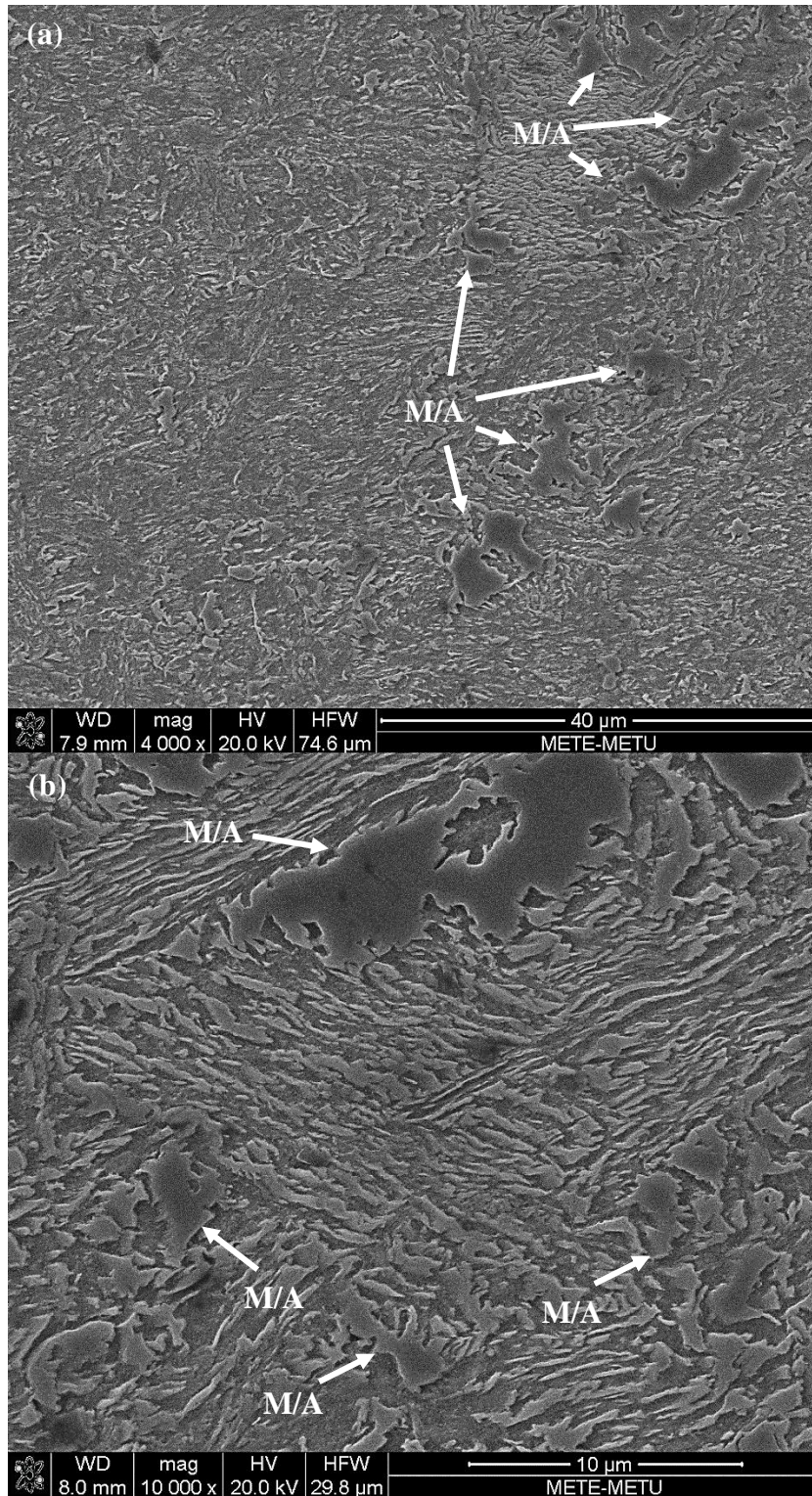
Figure 4.18. SEM micrographs of bainitic Cu-alloyed 4330M (a) at low magnification, (b) at high magnification, showing M/A constituents and carbide free bainitic matrix

SEM results of bainitic Cu-alloyed 4330M steel shows a mixture of bainite and M/A island similar to the 4330M that has gone through identical heat treatment. However, M/A islands in Cu-alloyed 4330M are chunkier and occupying a much bigger area than the ones found in 4330M steel as shown in Figures 4.16 and 4.18. This result also correlates well with the phase fraction results of optical micrographs where M/A phase fraction of Cu-alloyed 4330M bainitic steel is found higher than that of 4330M. Another difference is that the carbide precipitation among bainite sheaves cannot be observed even at higher magnifications in Cu-alloyed 4330M, as shown in Figure 4.19.
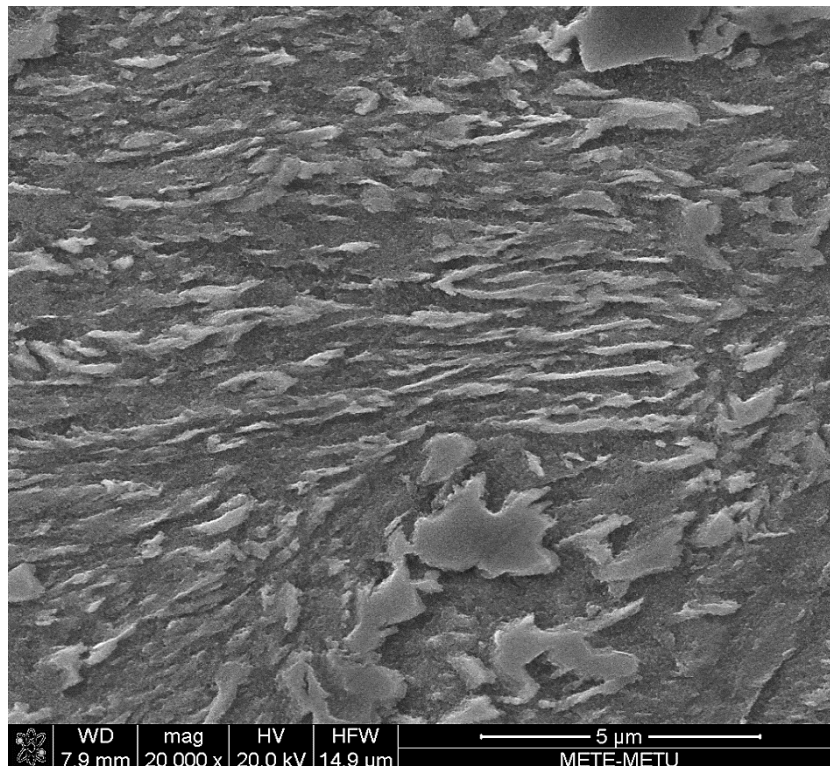
Figure 4.19. Carbide free bainitic matrix observed in bainitic Cu-alloyed 4330M, carbide precipitation cannot be seen.

4.2.3.2. Isothermally Transformed and Aged Microstructures

SEM metallographical examinations were also made after the aging of 4330M and Cu-alloyed 4330M bainitic steels. Carbide precipitation is observed in both steels, but with a difference in morphology. As shown in Figure 4.20, carbide precipitation at grain boundaries and needle shape carbides in bainitic matrix is observed for Cu-alloyed 4330M steel after it has been aged at 500°C for 90 minutes. Some amount of M/A constituent found in Cu-alloyed 4330M steel is also observed as decomposed M/A after aging treatment and, the fraction of M/A is decreased. Cementite precipitation at ferrite/austenite interface is also observed which is an evidence of the decomposition of austenite in M/A.
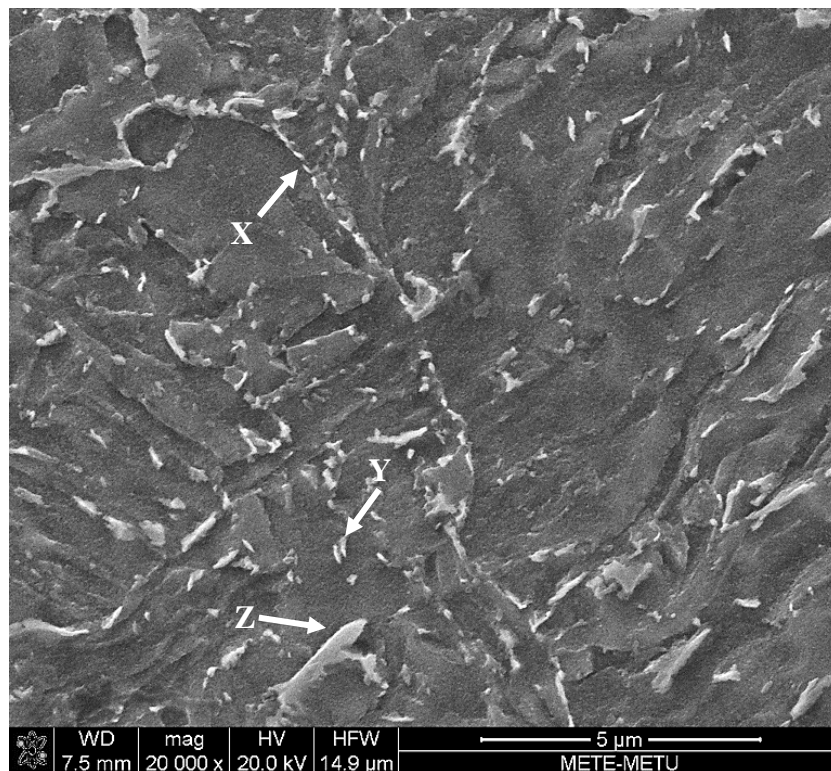
Figure 4.20. SEM micrographs of bainitic Cu-alloyed 4330M after aging at 500°C for 90 minutes, X; Carbide precipitation at austenite grain boundary, Y; Carbide precipitation at austenite grain boundary, Z; Cementite precipitation at α/γ interface.

Whereas for 4330M that has gone through the same heat treatment procedure, the shape and morphology of carbides are different. Coarser rounded shape or globular carbides are observed as shown in Figure 4.21.
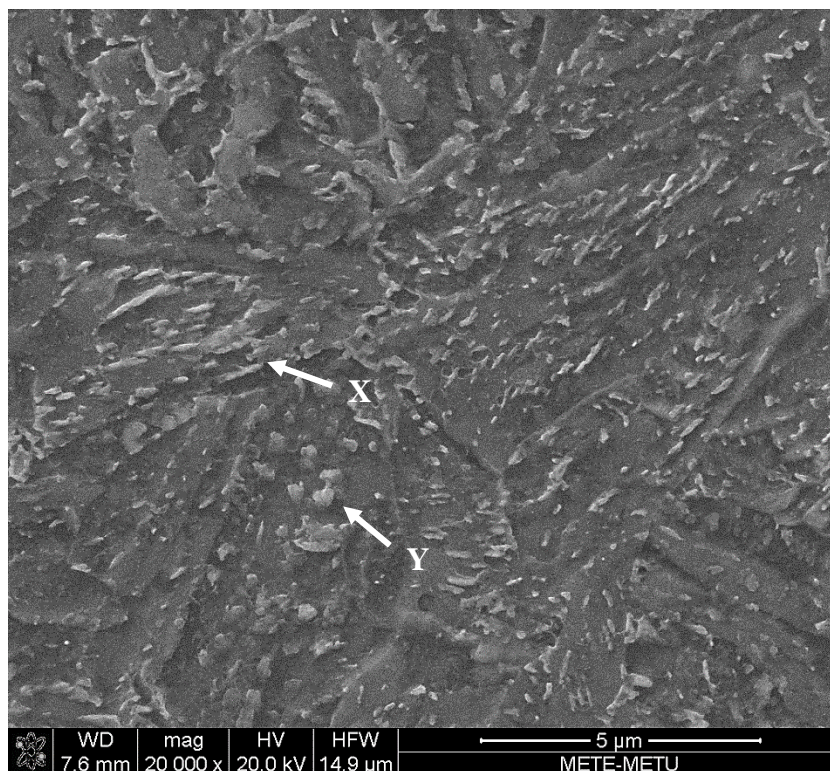
Figure 4.21. SEM micrographs bainitic 4330M after aging at 500°C for 90 minutes, X; rounded carbides, Y: globular carbides

4.3. Mechanical Test Results

4.3.1. Hardness Measurements

Table 4.4. *Hardness Test Results of As-Cast Steel*

Steel Type	HV30
4330M	327 ± 3
Cu-alloyed 4330M	374 ± 4

Hardness values of Cu-alloyed 4330M and 4330M are shown with Table 4.4. It can be seen that Cu-alloyed 4330M yields to higher hardness around 47 HV than 4330M steel in as-cast condition

4.3.2. Effect of Aging Temperature on Hardness for Martensitic and Bainitic Steels,

To determine the optimum aging temperature for copper precipitation, Cu-added and Cu-free, martensitic and bainitic steels are aged at different temperatures and hardness values are measured. For martensitic steels aging temperatures of 300°C, 400°C, 500°C, and 600°C were used. Bainitic steels were aged at 300°C, 400°C, 500°C, 550°C and 600°C. Aging time was kept constant at 90 minutes for all specimens and the hardness values are shown in Table 4.5 for martensitic samples and in Table 4.6 for bainitic samples.

Table 4.5. *Hardness Results vs Aging Temperature of Martensitic Steels*

Aging Temperature (°C)	Aging Time (min)	HV30	
		4330M	Cu-alloyed 4330M
As-Quenched		537 ± 7	524 ± 7
300		514 ± 2	505 ± 2
400	90	480 ± 3	478 ± 7
500		423 ± 5	454 ± 2
600		376 ± 7	383 ± 7

Table 4.6. *Hardness Results vs Aging Temperature of Bainitic Steels*

Aging Temperature (°C)	Aging Time (min)	HV30	
		4330M	Cu-alloyed 4330M
As-transformed		423 ± 5	418 ± 3
300		431 ± 3	423 ± 7
400	90	427 ± 1	429 ± 1
500		382 ± 3	428 ± 4
550		365 ± 2	403 ± 4
600		334 ± 5	381 ± 4

As seen from Table 4.5, for martensitic steels, the hardness values of the 4330M and Cu-alloyed 4330M steels do not differ much from each other with increasing tempering-aging temperature. Values steadily decrease with increasing aging temperature as a result of the tempering of the martensite except for the specimens at 500°C. Cu-alloyed 4330M yields higher hardness value, as shown in Figure 4.22, when aged at this temperature. Cu-alloyed 4330M steel is found to have 450 HV hardness, which is 30 HV higher than the 4330M steel which has undergone identical heat treatment procedures.
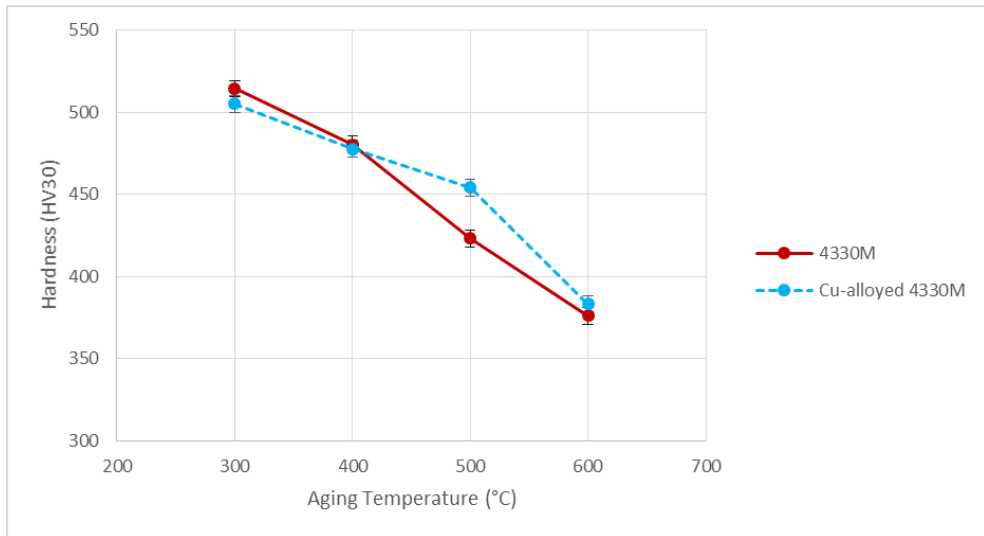
Figure 4.22. Hardness (HV30) vs. aging temperature (°C) graph for martensitic steels obtained by oil quench

For bainitic steels, the hardness values of the 4330M and Cu-alloyed 4330M steels differ from each other for aging temperatures above 400°C as shown in Figure 4.23. The difference in hardness is measured as 46 HV for 500°C, 38 HV for 550°C and 47 HV for 600°C. The retardation of softening effect is clearly seen when 4330M is alloyed with copper as the decrease in hardness was slowed down.
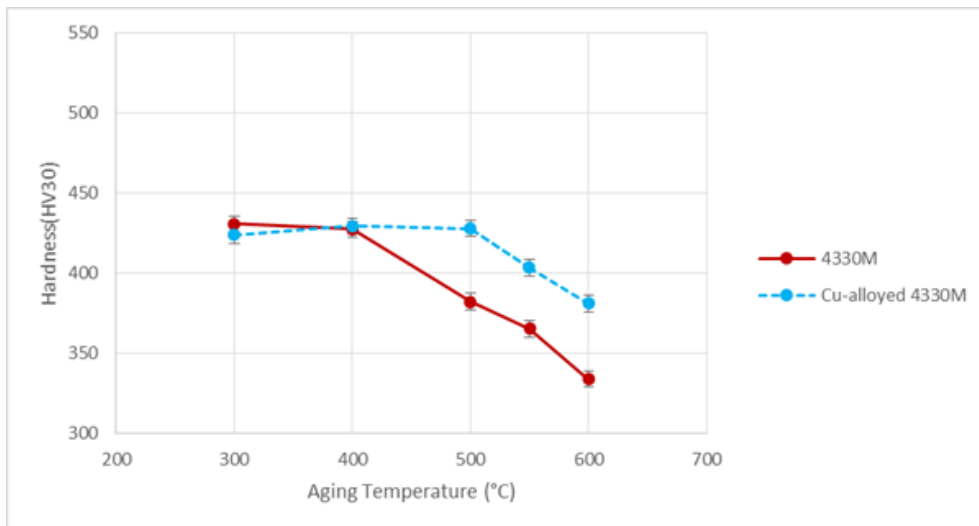
Figure 4.23. Hardness (HV30) vs aging temperature (°C) graph for bainitic steels

4.3.3. Effect of Aging Time on Hardness of Martensitic and Bainitic Steels

Effect of aging time on hardness for Cu-alloyed 4330M and 4330M steels were also investigated. Effect of aging time has been studied at 3 different temperatures, namely 450°C, 500°C and 550°C for both martensitic and bainitic steel samples. For obtaining bainitic and martensitic structure, the same type of heat treatment conditions that were used previously for aging temperature trials was used.

The results for martensitic Cu-alloyed 4330M and 4330M steels are shown in Table 4.7 and plotted in Figure 4.24.

Similar behavior by both steel types was observed with increasing aging time. Hardness decreased with increasing aging time for both 4330M and Cu-alloyed 4330M steel while retardation of softening effect of Cu is observed. Cu-alloyed 4330M yielded higher hardness values than 4330M at any aging time for different temperatures.

Table 4.7. *Hardness Results vs Aging Time of Martensitic Steels*

Steel Type	Aging Temp. (°C)	Hardness(HV30) at Aging Time(min)						
		0	10	60	90	180	270	360
4330M	450	537 ± 7	511 ± 3	442 ± 5	439 ± 4	435 ± 5	440 ± 2	439 ± 1
	500	537 ± 7	475 ± 5	447 ± 6	423 ± 5	433 ± 3	-	-
	550	537 ± 7	462 ± 3	442 ± 3	427 ± 3	414 ± 5	-	-
Cu-alloyed 4330M	450	524 ± 7	529 ± 4	469 ± 4	460 ± 1	482 ± 3	497 ± 2	490 ± 4
	500	524 ± 7	506 ± 2	476 ± 2	454 ±2	458 ± 2	-	-
	550	524 ± 7	490 ± 4	481 ± 4	447 ± 2	433 ± 5	-	-
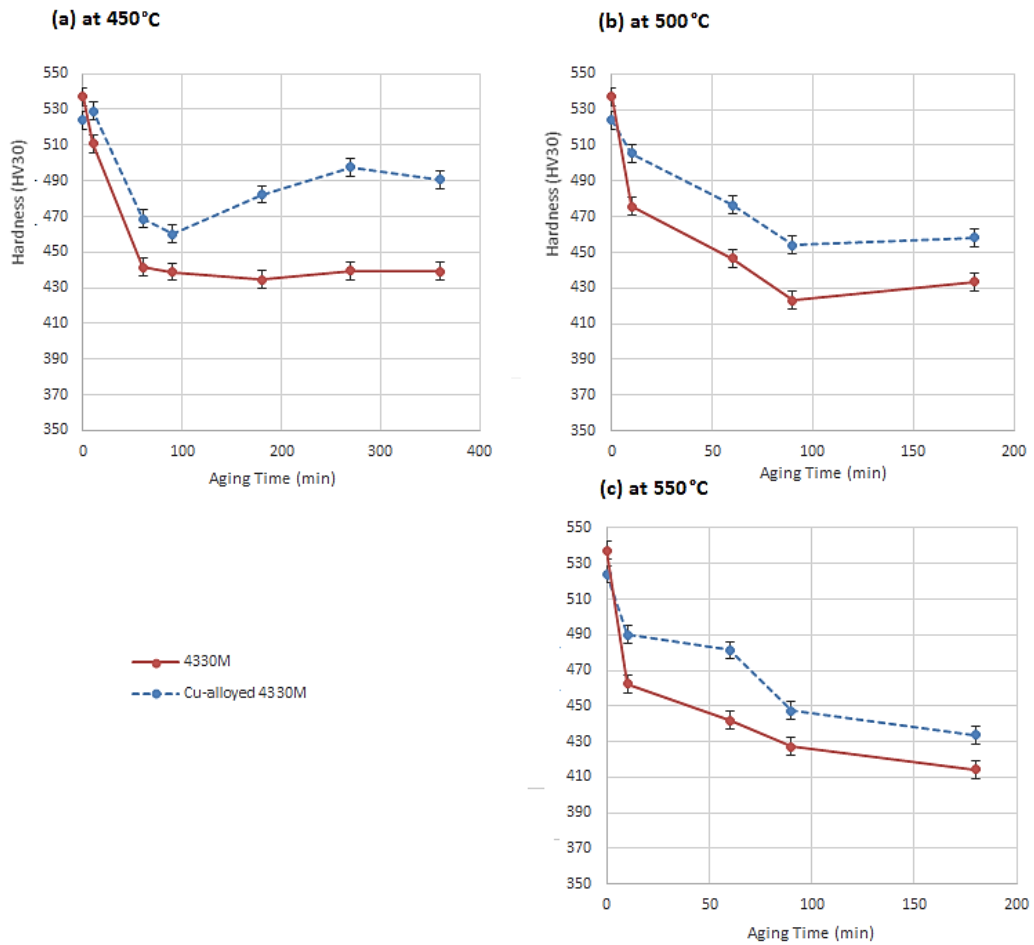
Figure 4.24. Hardness (HV30) vs aging time (min) graph for martensitic steels

The results for bainitic Cu-alloyed 4330M and 4330M steels are shown in Table 4.8 and Figure 4.25. An increase in hardness is observed for Cu-alloyed 4330M. Cu-alloyed 4330M values peaked at a particular time and then decreased with increasing time. Peak hardness is found to be 452 HV for 450°C at 270 minutes, 430 HV for 500°C for 60 minutes and 430 HV for 550°C at 10 minutes. Whereas for 4330M, hardness is decreased with increasing aging time and decrease in hardness is slowed down or reverted slightly after 90 minutes.

When the Cu-alloyed steels are considered, hardness values of martensitic specimens are higher than those of bainitic specimens.

On the other hand, it can be stated that the response of bainitic microstructure to aging is more sensitive than that of martensitic microstructure. The hardness of aged bainitic specimens exceeds that of un-aged ones. For example, the hardness of bainitic specimen after transformation is 418 HV but increases to 452 HV after aging treatment at 450°C for 270 minutes.

Table 4.8. *Hardness Results vs Aging Time of Bainitic Steels*

Steel Type	Aging Temp. (°C)	Hardness (HV30) at Aging Time(min)						
		0	10	60	90	180	270	360
4330M	450	423 ± 5	419 ± 2	403 ± 2	405 ± 2	395 ± 4	401 ± 2	400 ± 4
	500	423 ± 5	413 ± 4	394 ± 2	382 ± 3	389 ± 4	-	-
	550	423 ± 5	386 ± 2	372 ± 4	365 ± 2	364 ± 5	-	-
Cu-alloyed 4330M	450	418 ± 3	416 ± 3	425 ± 5	419 ± 2	438 ± 3	452 ± 1	446 ± 5
	500	418 ± 3	420 ± 4	439 ± 4	428 ± 4	425 ± 4	-	-
	550	418 ± 3	430 ± 3	411 ± 3	403 ± 4	400 ± 5	-	-
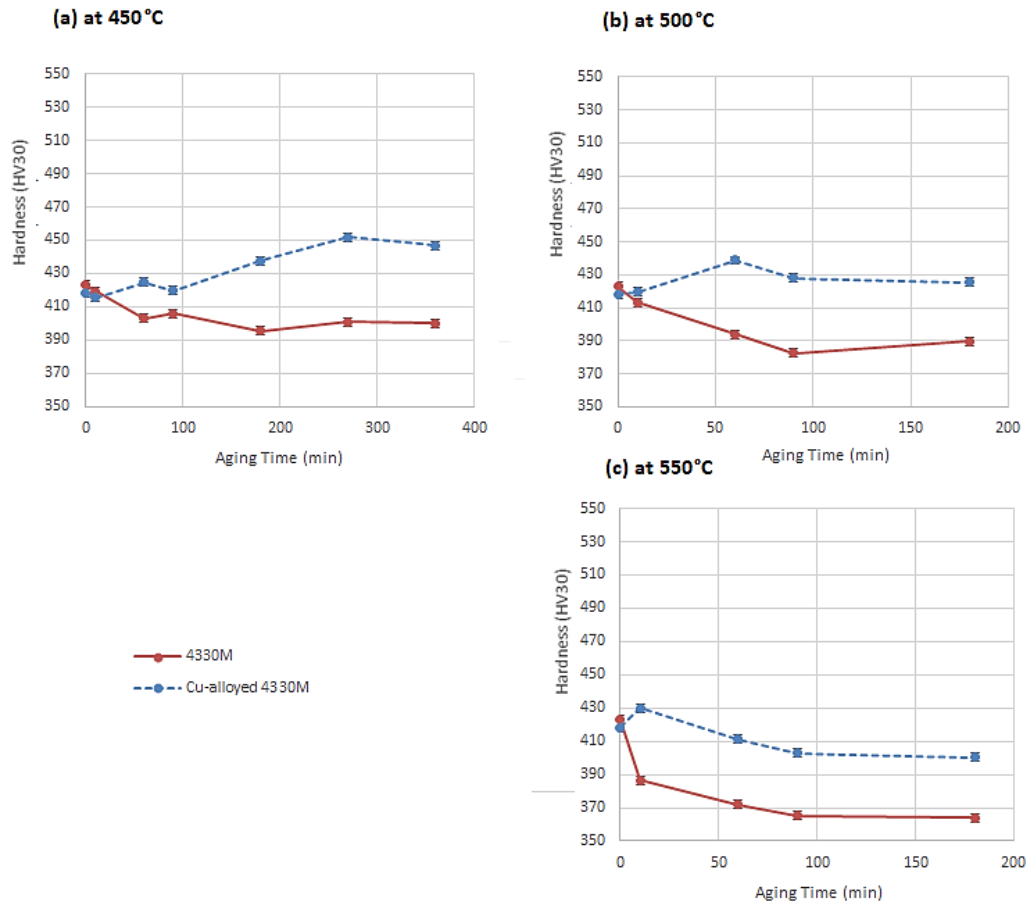
Figure 4.25. Hardness (HV30) vs. aging time (min) graph for bainitic steels

4.4. Tensile Testing and Fractography of Specimens

4.4.1. Tensile Testing

Table 4.9. *Tensile Test Results*

Steel Type	Transformation Type	Aging Temp. (°C) / Time (min)	Yield Stress (0.2% Offset (MPa)	Ultimate Tensile Stress (MPa)	Fracture Strain (%) Lo= 30mm
			Average		
Cu-alloyed 4330M	Bainitic	450 / 270	1204	1332	9.27
		550 / 60	1135	1369	8.65
	Martensitic	450 / 270	1357	1412	1.61
		550 / 60	1247	1334	6.79
4330M	Bainitic	450 / 270	1072	1170	1.22
		550 / 60	1158	1205	11.18
	Martensitic	450 / 270	1196	1303	5.21
		550 / 60	1138	1218	8.24

Tensile test was performed on two types of steel, heat-treated at 4 different conditions, thus a total of 8 conditions were tested. For each condition, two specimens were tested. The results shown in Table 4.9 are average values. Tensile stress vs tensile strain curves for the specimens which exhibited higher UTS values of the two specimens are shown in Figures 4.26 and 4.27.

The highest ultimate tensile strength of 1412 MPa is observed for martensitic Cu-alloyed 4330M specimens aged at 450°C for 270 minutes which also has the greatest yield strength, 1357 MPa.

On the other hand, bainitic 4330M specimens aged at 550°C for 60 minutes provided the highest tensile strain, 11.18 %.

At every condition, Cu-alloyed 4330M resulted in greater yield strength and tensile strength values than those of 4330Ms.

When the tensile test curves are examined, ductile type fracture is observed for all but martensitic Cu-alloyed 4330M and bainitic 4330M steel samples aged at 450°C for 270 minutes. Premature fracture is observed for specimens at these two conditions.
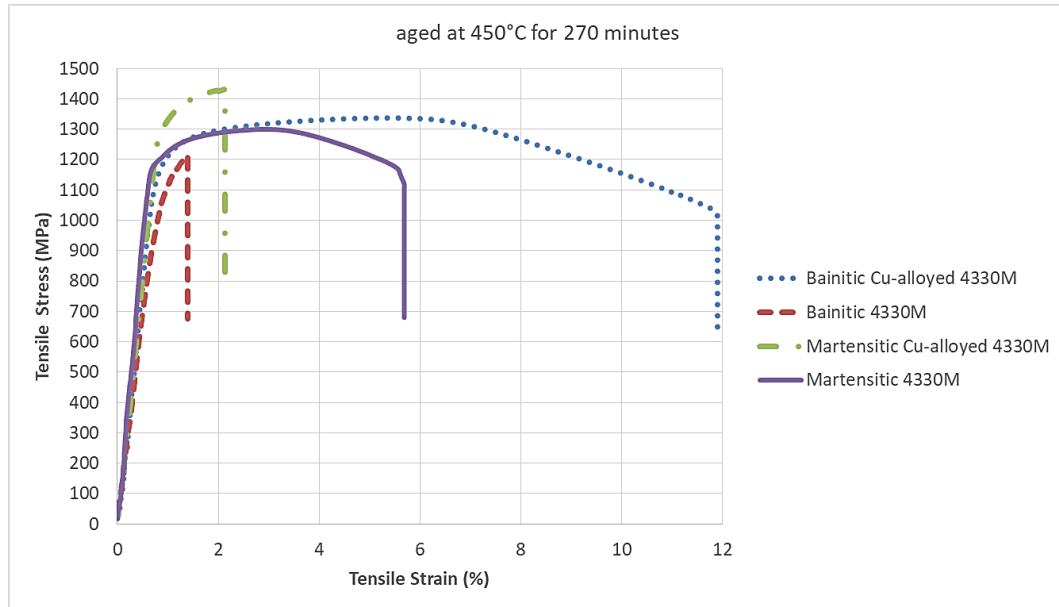
Figure 4.26. Tensile Stress (MPa) vs tensile strain (%) graph for bainitic and martensitic steels (specimens with higher UTS) after aging at 450°C for 270 minutes
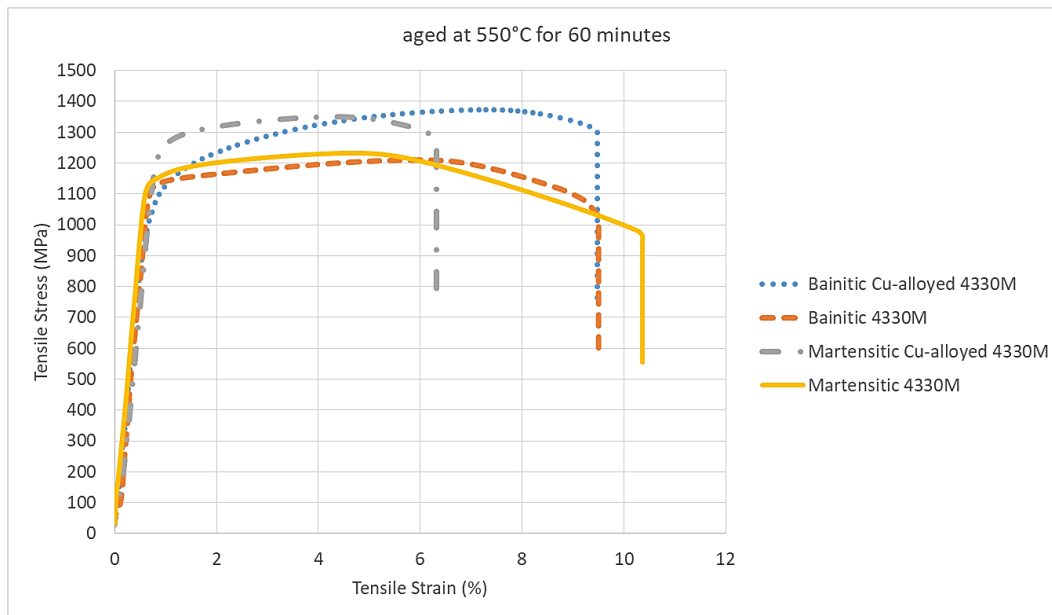
Figure 4.27. Tensile Stress (MPa) vs Tensile Strain (%) graph for bainitic and martensitic steels (specimens with higher UTS) after aging at 550°C for 60 minutes

4.4.2. Fractography Results

Fracture surfaces of tensile specimens belonging to 8 conditions were examined at SEM. Fractographs are shown in Figure 4.28 – 4.37.

Ductile fracture features were observed for 5 conditions except following 3 conditions;

- Martensitic Cu-alloyed 4330M aged at 450°C for 270 minutes
- Bainitic 4330M steel samples aged at 450°C for 270 minutes
- Martensitic Cu-alloyed 4330M after aging at 550°C for 60 minutes

For these three conditions, brittle fracture dominant mixed fracture surfaces were observed at SEM.
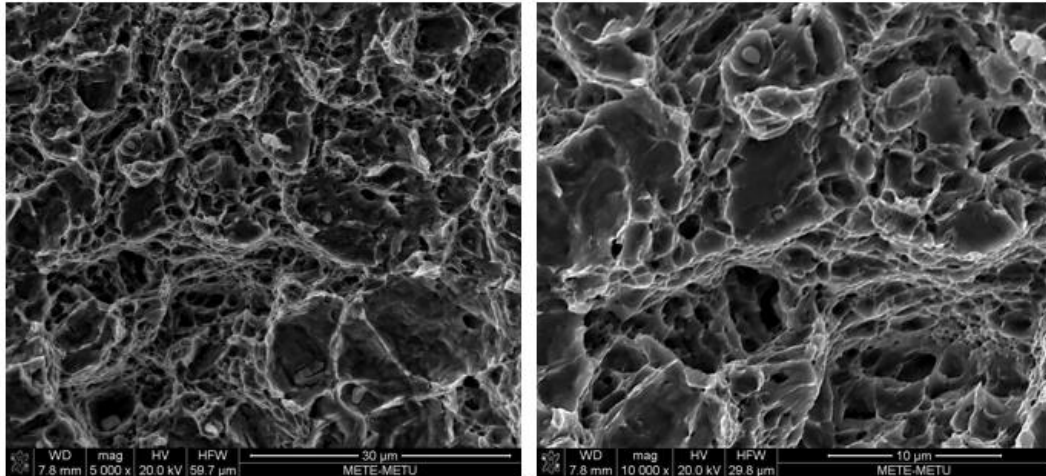
Figure 4.28. SEM fractography of the tensile specimen of martensitic 4330M after aging at 450°C for 270 minutes showing almost fully ductile fracture behavior.
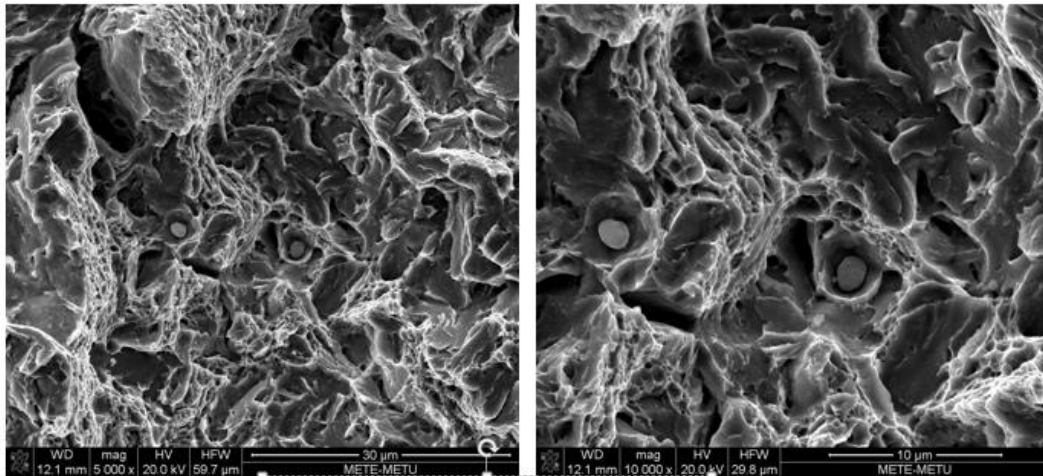
Figure 4.29. SEM fractography of the tensile specimen of martensitic Cu-alloyed 4330M after aging at 450°C for 270 minutes showing mixed type fracture behavior, both dimples and cleavage planes are seen.
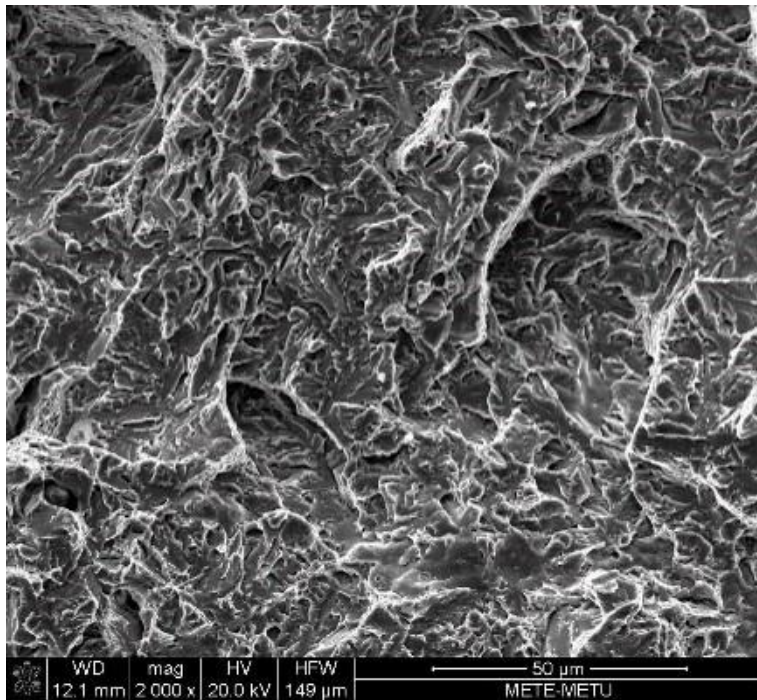
Figure 4.30. SEM fractography of the tensile specimen of martensitic Cu-alloyed 4330M after aging at 450°C for 270 minutes at lower magnification showing mainly brittle type of fracture behavior characteristics, the dimples can be observed at higher magnifications as shown with Figure 4.27.
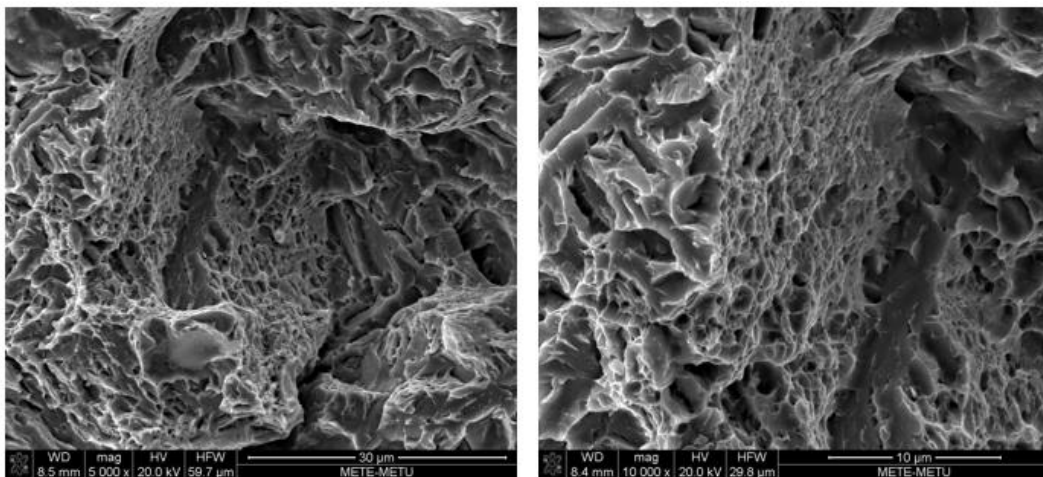
Figure 4.31. SEM fractography of the tensile specimen of bainitic 4330M after aging at 450°C for 270 minutes showing mixed type fracture behavior, both micro dimples and cleavage planes can be observed.
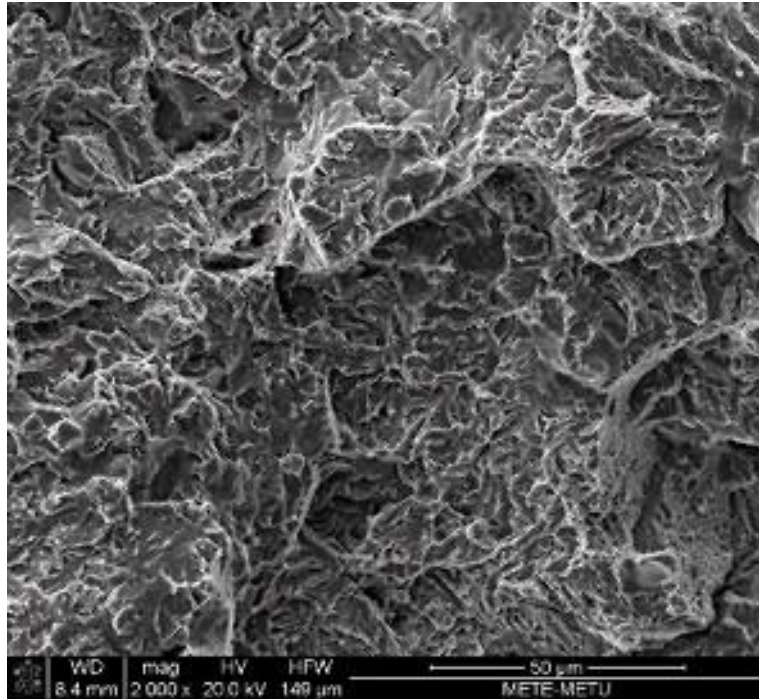
Figure 4.32. SEM fractography of the tensile specimen of bainitic 4330M after aging at 450°C for 270 minutes at lower magnification showing mainly brittle type fracture characteristics, the dimples can be observed at higher magnifications as shown with Figure 4.29.
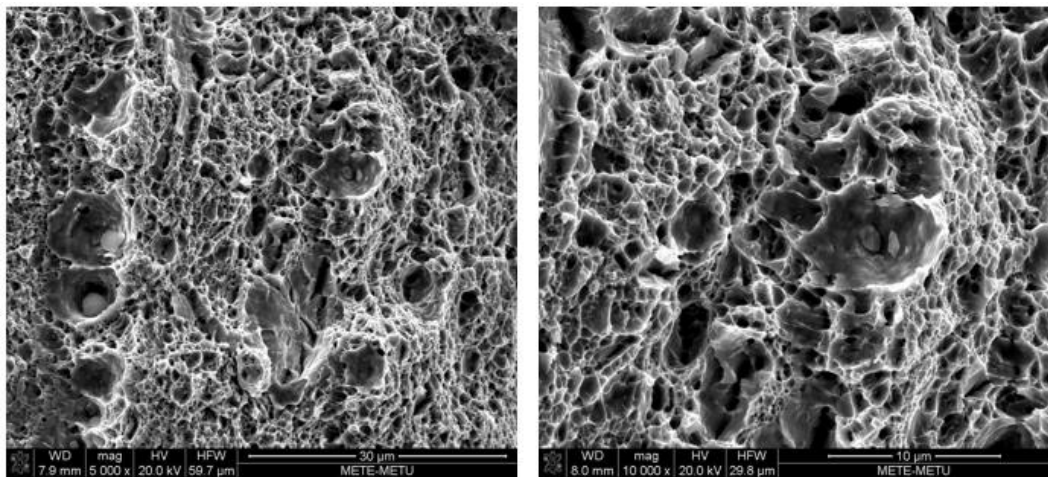
Figure 4.33. SEM fractography of the tensile specimen of bainitic Cu-alloyed 4330M after aging at 450°C for 270 minutes, showing ductile fracture behavior as fracture surface is composed of dimples.
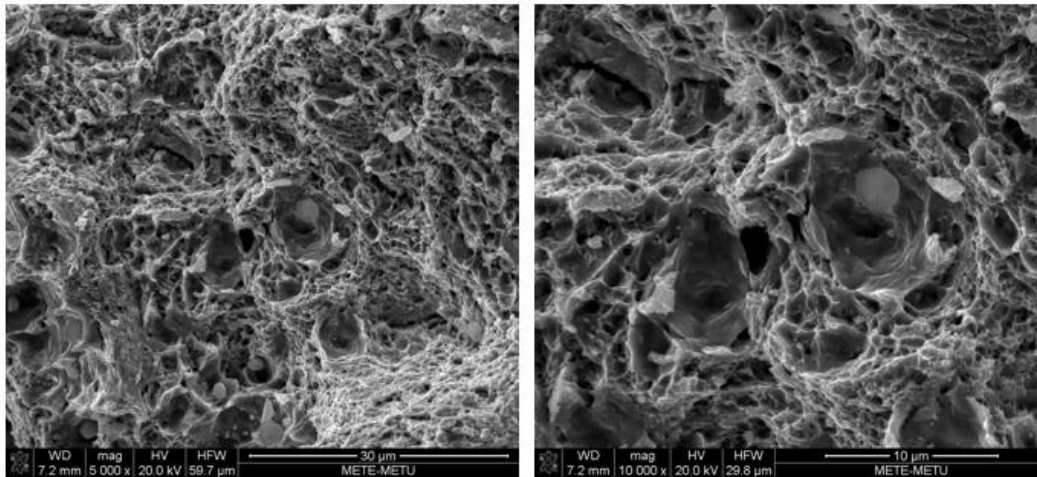
Figure 4.34. SEM fractography of the tensile specimen of martensitic 4330M after aging at 550°C for 60 minutes showing ductile type fracture with dimples.
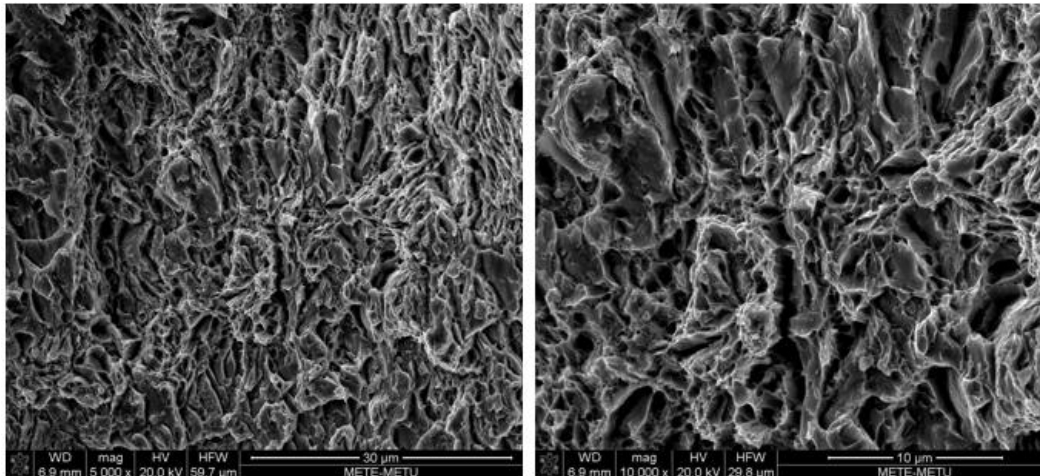
Figure 4.35. SEM fractography of the tensile specimen of martensitic Cu-alloyed 4330M after aging at 550°C for 60 minutes showing mixed type chracteristics with typical quasi-cleavage type fracture surface.
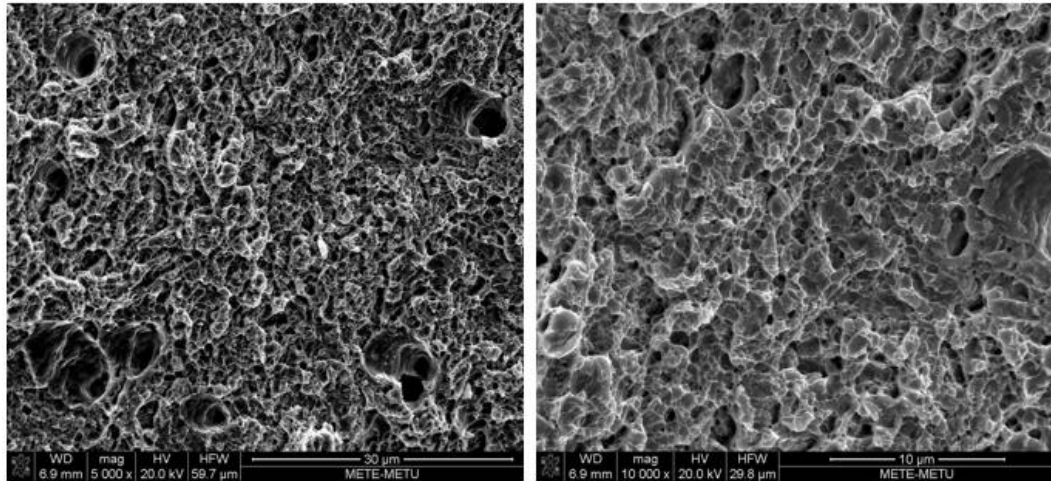
Figure 4.36. SEM fractography of the tensile specimen of bainitic 4330M after aging at 550°C for 60 minutes showing ductile type fracture behavior, inclusion decohesion and growth of cavities are also observed
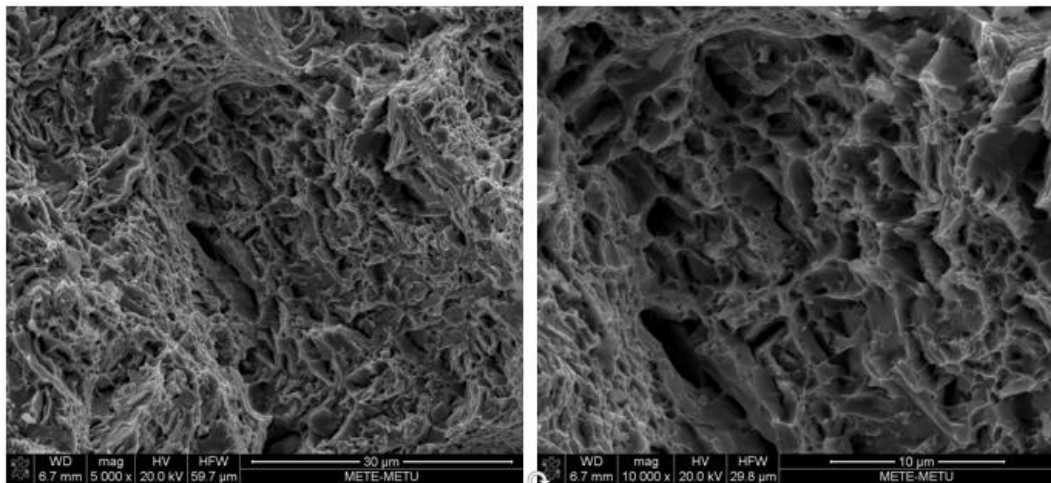
Figure 4.37. SEM fractography of the tensile specimen of bainitic Cu-alloyed 4330M after aging at 550°C for 60 minutes showing mixed type fracture behavior, dimples can be observed.

CHAPTER 5

DISCUSSIONS

5.1. Effect of Copper on As-Cast Steel Properties

As-cast morphologies of both 4330M and Cu-alloyed 4330M were similar. The morphology was expected to be a mixture of pearlite and pro-eutectoid ferrite since the carbon content of steels is around 0.28 wt%, which is lower than eutectoid composition and steel is cooled in air. However, the expected microstructure in which there is pro-eutectoid ferrite on grain boundaries and pearlite in grains was not obtained in optical micrographs because of the dendritic solidification characteristics observed in as-cast microstructures.

The microstructure of both steel was found as a mixture of ferrite and pearlite from SEM micrographs. The ferrite is identified as pro-eutectoid ferrite since both steel is hypo-euctectoid. Phase fraction analysis of SEM micrographs have shown that the phase ratio of pearlite in Cu-alloyed 4330M was 30% higher than that of 4330M.

As-cast Cu-alloyed 4330M had shown about 47 HV higher hardness value. This can be related to the difference in the pearlite phase ratio. Since pearlite is a harder phase than ferrite, a higher amount of pearlite leads to a higher hardness. Another reason could the difference in the pearlitic structure of steels. As mentioned in earlier chapters; copper is an austenite stabilizer which means that the austenite to pearlite formation eutectoid transformation occurs at a lower temperature when copper addition is done to steel. When the transformation occurs at lower temperatures, the inter-lamellar spacing between cementite and ferrite of pearlite phase becomes smaller due to lowered diffusion rate. This smaller inter-lamellar spacing leads to a finer structure that is related to the increase in hardness.

5.2. Effect of Copper on Bainitic Steel Properties

When microstructural features of isothermally treated steels, both 4330M and Cu-alloyed 4330M are examined, it can be stated that for both alloy, the microstructure is composed of bainite and M/A islands. However, phase fraction of M/A in Cu-alloyed 4330M is found to be four times more than that of 4330M. The difference in the phase fractions can be explained with the cementite suppression effect of Cu. As described previously, Cu suppresses cementite formation during bainitic transformation thus the carbon in newly formed ferrite goes into neighboring austenite and the neighboring austenite becomes enriched by carbon. This leads to a decrease in martensite start temperature and also delays bainitic transformation. Thus a retained austenite is found among bainite which may transform to martensite after bainitic transformation has been completed if the ambient temperature is lower than martensite finish temperature. If it is between M_s and M_f, a mixture of retained austenite and martensite is formed. This is presumably the case observed in this study.

SEM results are in line with the optical microscopy examinations as expected. The ratio M/A island was higher in Cu-alloyed 4330M and the islands were bulkier in form. Another difference was in terms of carbide-cementite precipitation. Carbide precipitation was non-existing in Cu-alloyed 4330M while it was clearly observed in 4330M. The reason behind these two differences can be expressed by the cementite suppression effect of Cu. This effect is the result of copper's low solubility in cementite which results in trapping of Cu at cementite boundaries and reducing the driving force for cementite precipitation, which also contributes to increase in fraction of M/A islands as stated before.

Aged microstructures of bainitic steels were also investigated under SEM, which have shown that while carbide precipitation is obtained for both steel type, they are distinguished in terms of the morphology of carbides. Needle-shaped carbides are seen in aged Cu-alloyed 4330M bainitic steel, whereas coarser rounded shape or globular carbides exist in 4330M. The needle shape carbides are formed during aging while

globular shape carbides found in 4330M are probably the carbides exist prior to aging, which have grown and become rounded during aging. M/A constituent observed in Cu-alloyed 4330M is mostly decomposed as described in the study of Podder et al. that austenite can decompose into precipitates of cementite and ferrite along bainitic ferrite and austenite interface [44].

When hardness values of bainitic Cu-alloyed 4330Ms are considered, an increase in hardness at each of 450°C, 500°C and 550°C were observed in contrast to the 4330M alloy where steady decrease in hardness is reported. The increase was 34 HV for 270 minutes at 450°C, 21 HV for 60 minutes at 500°C and 12 HV for 10 minutes at 550°C aging times and temperatures.

In addition to increase in hardness observed in bainitic steels, when the hardness values of 4330M and Cu-alloyed 4330Ms are compared as shown in Figure 5.1, effect of copper is seen more clearly. It is seen that the highest difference in hardness between two types of steel is 51 HV for 450°C at 270 minutes, 46 HV for 500°C at 90 minutes and 44 HV for 550°C at 10 minutes aging temperatures and times.

The difference in hardness of aged 4330M and Cu-alloyed 4330Ms bainitic steels can be explained by copper precipitation strengthening mechanism and copper's effect on microstructure since the only different condition between these two alloy is the addition of copper.
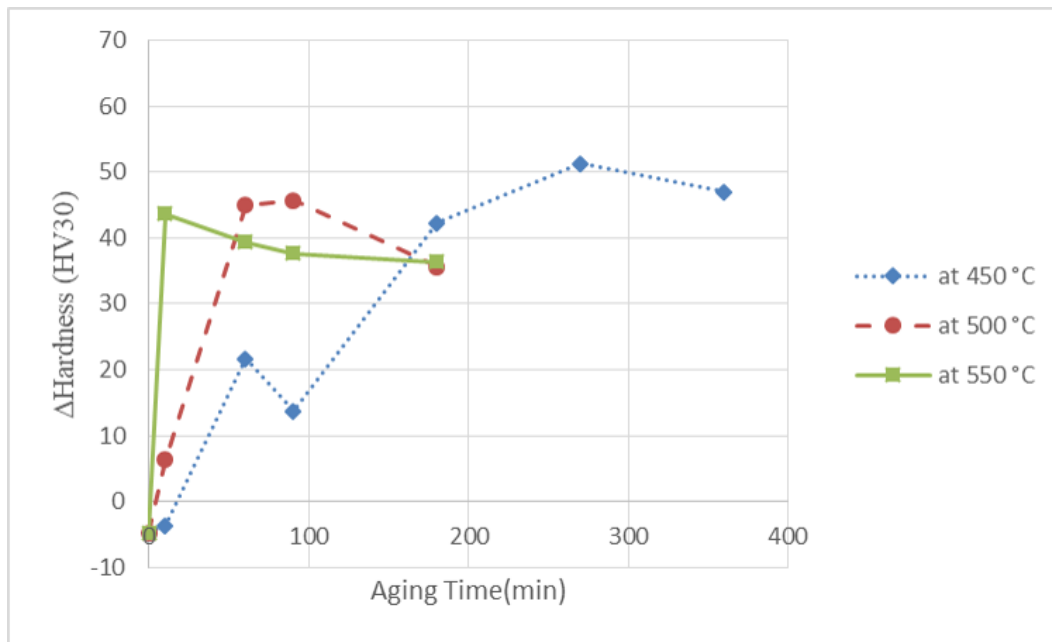
Figure 5.1. Hardness (HV30) vs. aging time (min) for bainitic steels ΔHardness refers to the difference in hardness values of Cu free and Cu added steels at different time and temperature.

Since Cu precipitates need to reach a critical size of 2-3 nm to show the effect of precipitation strengthening, then for each temperature a different aging time is required to reach the highest hardness or to observe the peak hardness difference between 4330M and Cu-alloyed 4330M. It is clearly observed that as the temperature increases, peak hardness is reached at shorter aging times.

Tensile test results are found to be supporting hardness results as Cu-alloyed 4330M bainitic steels have a higher yield and tensile strength values than those of 4330M after aging at two different temperatures. The difference of UTS in favor of Cu-alloyed 4330M was 162 MPa for aging at 450°C for 270 minutes while it was up to 164 MPa for aging at 550°C for 60 minutes.

The improvements in hardness, yield and tensile strength are believed to be related with the existence of copper precipitates induced strengthening mechanism as other studies in literature indicated a positive effect of these precipitates on mechanical

properties after aging around 450-500°C. The other reason could be the change in microstructure of bainitic steels triggered by Cu addition. One of the effects of Cu addition on microstructure was suppression of cementite in bainite sheaves which resulted in the change in the morphology of carbides found in aged bainite. Carbide found in aged state of Cu-alloyed 4330M bainitic steel are finer and needle shaped whereas the ones found in 4330M bainitic steel that are coarser and have spherical morphology which are less effective in increasing strength and hardness of steels. That's why the difference in the morphology of carbides could be accounted for, beside copper precipitation, as another reason for higher yield strength, UTS and hardness found in Cu-alloyed 4330M.

In terms of tensile strain, aging at 550°C for 60 minutes resulted in similar findings between Cu-alloyed 4330M and 4330M. On the other hand, for aging at 450°C for 270 minutes, Cu-alloyed 4330M yielded 9.27% tensile strain while 4330M prematurely fractured at 1.22% strain. This premature fracture might be related to the casting defects such as gas porosity and shrinkage porosity caused by dendritic solidification.

5.3. Effect of Copper on Martensitic Steel Properties

The microstructures of 4330M and Cu-alloyed 4330M martensitic steels were found to be similar as optical microscopy and SEM micrographs illustrated no notable difference in morphology of martensite as-quenched state or after aging, which can be read as Cu has shown no effect on martensitic transformation and tempering of martensite.

On the contrary to microstructural investigations the mechanical properties of 4330M and Cu-alloyed 4330M martensitic steel differ from each other as hardness and tensile tests indicated.

71
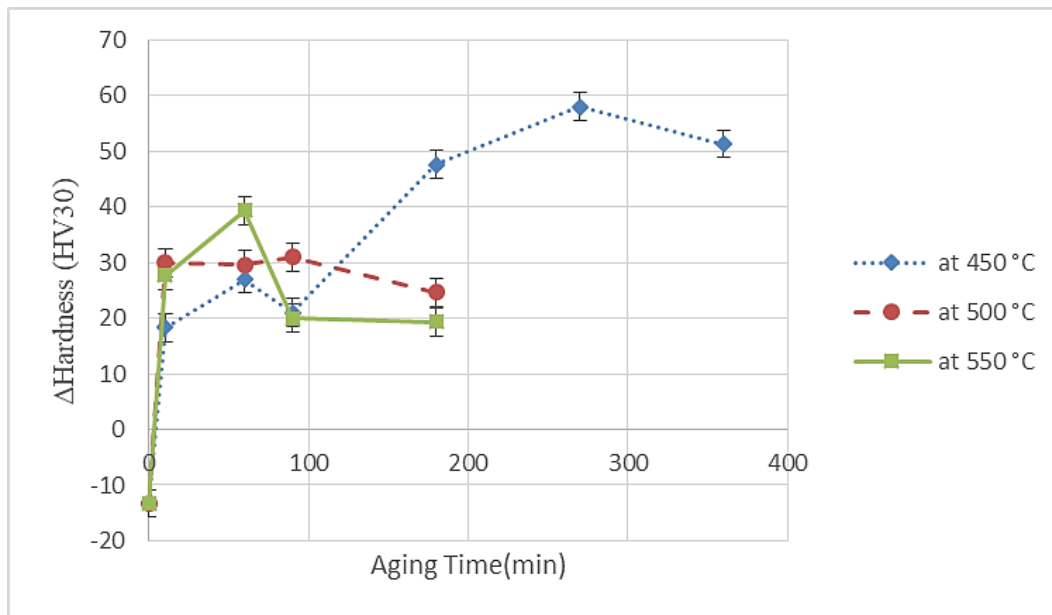
Figure 5.2. ΔHardness (HV30) vs. aging time (min) for martensitic steels. ΔHardness refers to difference in hardness values of Cu free and Cu added steels at different aging time and temperature

When hardness values of Cu-alloyed 4330M and 4330M martensitic steel aged at different temperatures are examined as shown in Figure 5.2 which simply indicates ''hardness differences between Cu-alloyed 4330M and 4330M'' at various aging temperatures, it is seen that Cu-alloyed 4330M yielded higher hardness values than those of 4330M at every aging temperature. It is also seen that the highest difference in hardness is 57 HV for 450°C at 270 minutes, 31 for 500°C at 90 minutes and 39 HV for 550°C at 90 minutes aging times and temperatures.

Similar to hardness results, Cu-alloyed 4330M also resulted in higher yield and ultimate tensile strength values than 4330M. Cu-alloyed 4330M martensitic steel provides up to 116 MPa higher UTS value as compared to 4330M when aged at 550°C for 60 minutes, whereas it was 109 MPa for aging at 450 °C for 270 minutes. The differences in yield strength, tensile strength and hardness are most probably due to the presence of Cu precipitates that have supersaturated during quenching and reach critical size with aging as in the case of bainitic steels. Since the microstructures of

both 4330M and Cu-alloyed 4330M are similar after aging as shown in the experimental results, the difference can be related to the sole effect of Cu precipitates, which cannot be observed under optical and SEM microscopy since their size is in nanometer scale.

In the case of tensile strain, the results were similar for Cu-alloyed 4330M and 4330M martensitic steel aged at 550°C for 60 minutes. In contrast with this, results differed between two steel types for aging at 450°C for 270 minutes with 1.61% for Cu-alloyed 4330M and 5.21% for 4330M. However Cu-alloyed 4330M that 1.61% tensile strain observed is thought to fracture prematurely with brittle fracture as shown in fractography results because of defects found in cast steel, which may express limited tensile strain.

5.4. Difference in Aging Responses of Bainitic and Martensitic Steels

Tensile test specimens of Cu-alloyed 4330 martensitic steel responded to increased aging temperature differently than bainitic steels.

UTS of martensitic steel specimens dropped down to 1334 MPa from 1412 MPa when aging temperature is increased from 450°C to 550°C.

On the other hand, UTS of bainitic steels remained at the similar level with 1332 MPa at 450°C and 1369 MPa at 550°C which is even higher than the UTS of martensitic steel at the same aging temperature.

This can be explained with decreasing effect of carbon solid solution strengthening due to formation of carbide precipitates during initial stage of aging/tempering and growth of these carbides during the later stages of tempering. This phenomenon is not observed during the aging of bainite. Thus with the strengthening effect of Cu precipitates, bainitic steel is believed to respond aging in a better way in terms of UTS.

Same case is also valid for hardness with increasing aging time for martensitic and bainitic Cu-alloyed 4330 steels. As the hardness of martensitic steels decreases with increasing aging time, bainitic steel is affected to lesser degree by aging time. Even

an increase in hardness is observed in bainitic steels after aging which is most likely related to copper precipitation strengthening. This difference in behavior can also be related to the distinctive effects of tempering/aging on martensite and bainite phases as mentioned previously.

CHAPTER 6

CONCLUSIONS

This study aimed at identifying the effects of copper on aging characteristics of a medium-carbon steel. To understand the effects, copper-free 4330M and copper-alloyed 4330M versions of a cast steel alloys were prepared which were then subjected to various heat treatments and then the results of these two steels were compared in terms of microstructure, hardness, tensile test and fractography. The following conclusions can be drawn from the results of the work performed in this thesis;

1. Cu addition is identified to have an impact in bainitic transformation characteristics in terms of cementite formation. It leads to suppression of cementite which results in an increase in the phase fraction of M/A (martensite/austenite) constituent. The fraction of M/A is found as 2.5% for 4330M while it is 13.0% for Cu-alloyed 4330M. Suppression of cementite could not be maintained after subsequent aging and the formation of needle-shaped cementite is observed.

2. Hardness increases in Cu-alloyed 4330M bainitic steels upon aging at 450°C, 500°C and 550°C while aging resulted in decrease in hardness for 4330M bainitic steels. The highest hardness value observed is 452 HV for Cu-alloyed 4330M bainitic steel when aged at 450°C for 270 minutes while the hardness value of 4330M at the same condition is 401 HV. Furthermore, upon aging at 550°C for 60 minutes, Cu-alloyed 4330M bainitic steel is found to have a UTS value of 1369 MPa which is 160 MPa higher than that of 4330M.

3. Cu addition yields no significant change in morphology of martensite in both alloys. 4330M and Cu-alloyed 4330M have similar microstructure in terms of martensite morphology after oil quenching. However, retardation of softening effect is observed as Cu-alloyed 4330M results in up to 60 HV higher hardness than 4330M when both steel are aged at 450°C for 270 minutes. In addition to that, after same aging process, Cu-alloyed 4330M martensitic steel has yielded an UTS value of 1412 MPa which is approximately 100 MPa higher than that of 4330M.

4. With increasing aging time, a peak hardness which is even higher than that of un-aged specimens is observed Cu-alloyed 4330M bainitic steels whereas no peak hardness is observed for Cu-alloyed 4330M martensitic steels, which is most probably due to different response of these phases to aging/tempering treatment.

REFERENCES

[1]Ardell, A. J. (1985). Precipitation hardening. Metallurgical Transactions A, 16(12), 2131–2165. doi: 10.1007/bf02670416

[2]Heat Treating, Vol 4, ASM Handbook, ASM International, 1991

[3]Babu, P. N., Satyanarayana, M. V. N. V., & Reddy, M. G. S. (2016, January 1). Effect of Aging on Mechanical Properties of S465 Stainless Steel. International Journal for Research in Applied Science & Engineering Technology (IJRASET), 4(1), 301–306.

[4]Bai, X.-M., Ke, H., Zhang, Y., & Spencer, B. W. (2017). Modeling copper precipitation hardening and embrittlement in a dilute Fe-0.3at.%Cu alloy under neutron irradiation. Journal of Nuclear Materials, 495, 442–454. doi: 10.1016/j.jnucmat.2017.08.042

[5]Imai, N., Komatsubara, N., Kunishige, N. Effect of Cu and Ni on hot workability of hot-rolled mild steel. ISIJ Int. 37 (1997), 224–23

[6]F. C. Campbell, Elements of metallurgy and engineering alloys. ASM International, 2008

[7]Fourlaris, G., & Baker, A. J. (1997). Bainite Formation in High Carbon Copper Bearing Steels. Le Journal De Physique IV, 07(C5). doi: 10.1051/jp4:1997561

[8]Ławrynowicz, Z. (2012). An investigation of the mechanism of bainite transformation in experimental 0.2c-1v-2mn steel. Advances in Materials Sciences, 12(2). doi: 10.2478/v10077-012-0005-4

[9]Bhadeshia, H. K. D. H. (2019). Bainite in Steels. doi: 10.1201/9781315096674

[10] Ławrynowicz, Z. (2004). Transition from upper to lower bainite in Fe–C–Cr steel. Materials Science and Technology, 20(11), 1447–1454. doi: 10.1179/026708304x3953

[11] C.N. Hisao & J. R. Yang, Age Hardening in Martensitic/Bainitic Matrices in a Copper-Bearing Steel, Material Transaction, 41(8): 1312-1321, 2000.

[12] W. L. Costin, O. Lavigne, and A. Kotousov, "A study on the relationship between microstructure and mechanical properties of acicular ferrite and upper bainite," Mater. Sci. Eng. A, vol. 663, pp. 193–203, 2016.

[13] H. Bhadeshia and R. Honeycombe, Steels: Microstructure and Properties, 4th ed. Elsevier Ltd, 2017.

[14] Bhadeshia. (2013). About Calculating The Characterics of the Martensite-Austeniste Constituent, 99–106.

[15] He, B., Xu, W., & Huang, M. (2015). Effect of ausforming temperature and strain on the bainitic transformation kinetics of a low carbon boron steel. Philosophical Magazine, 95(11), 1150–1163. doi: 10.1080/14786435.2015.1025886

[16] F. C. Campbell, "Non-equilibrium Reactions—Martensitic and Bainitic Structures," 2012, pp. 303–338.

[17] Yongqiang, H., Guoli, X., & Guoli, Y. (2018). Study on martensite strengthening mechanism and phase transition. Insight - Mechanics, 33–39.

[18] Zemui, S. (2017). Faculty of Health, Science and Technology.

[19] Introduction to Steel Heat Treatment. (2013). Steel Heat Treating Fundamentals and Processes, 3–25. doi: 10.31399/asm.hb.v04a.a0005819

[20] Chang, Shoulu, The second stage of tempering, Master of Engineering thesis, Department of Materials Engineering, University of Wollongong, 1994. https://ro.uow.edu.au/theses/2388

[21]Kimura, Y. & Takaki, S. 1997. Phase transformation mechanism of Fe-Cu alloys, ISIJ International 37: 290-295.

[22]Deschamps, A., Militzer M. & Poole, w.J. 2001. Precipitation kinetics and strengthening of a Fe 0.8wt%Cu alloy, ISIJ International 41: 196-205.

[23]Takaki, S., Fujioka, M., Aihara, S., Nagataki, Y., Yamashita, T., Sano, N.Yaguchi, H. (2004). Effect of Copper on Tensile Properties and Grain-Refinement of Steel and its Relation to Precipitation Behavior. Materials Transactions, 45(7), 2239-2244. doi:10.2320/matertrans.45.2239

[24]Perez, M., Perrard, F., Massardier, V., Kleber, X., Deschamps, A., Monestrol, H. D., Covarel, G. (2005). Low-temperature solubility of copper in iron: experimental study using thermoelectric power, small angle X-ray scattering and tomographic atom probe. Philosophical Magazine,85(20), 2197-2210. doi:10.1080/14786430500079645

[25]Ormston, D., Schwinn, V., & Hulka, K. (2005). Development of Low Carbon Microalloyed Bainitic Steels for Structural Plate Applications. Materials Science Forum, 500-501, 573–580. doi: 10.4028/www.scientific.net/msf.500-501.573

[26]M. Maalekian, (2007). The Effects of Alloying Elements on Steels. Christian Doppler Laboratory for Early Stages of Precipitation.

[27] Hongliang, Y. (2010). Pohang University of Science and Technology, Pohang.

[28] Stepanova, N., Zimogliadova, T., Ognev, A., Krivizhenko, D., Maliutina, Y., & Zimogliadova, O. (2017). Effect of copper on the structure and antifriction properties of cast hypoeutectoid steel. IOP Conference Series: Materials Science and Engineering, 286, 012024. doi: 10.1088/1757-899x/286/1/012024

[29]Kozeschnik, E., & Bhadeshia, H. (2008). Influence of silicon on cementite precipitation in steels. Material Science and Technology, 24(3), 343-348. doi:10.1179/174328408X275973

[30]Bhadeshia, H. K. D. H. (2019). Cementite. International Materials Reviews, 1–27. doi: 10.1080/09506608.2018.1560984

[31]Duparc, H. A. H., Doole, R. C., Jenkins, M. L., & Barbu, A. (1995). A high-resolution electron microscopy study of copper precipitation in Fe-1.5 wt% Cu under electron irradiation. Philosophical Magazine Letters, 71(6), 325–333. Doi:10.1080/09500839508241015

[32]Maruyama, N., Sugiyama, M., Hara, T., & Tamehiro, H. (1999). Precipitation and Phase Transformation of Copper Particles in Low Alloy Ferritic and Martensitic Steels. Materials Transactions, JIM,40(4), 268-277. doi: 10.2320/matertrans1989.40.268

[33]Vaynman, S., Fine M., Asfahani, R., Bormet, D., Hahin, C. (2002). High Performance Copper-Precipitation-Hardened Steel, Material Solutions Conference.2002.

[34]Bhagat, A. N., Pabi, S. K., Ranganathan, S., & Mohanty, O. N. (2004). Aging Behavior in Copper Bearing High Strength Low Alloy Steels. ISIJ International, 44(1), 115–122. doi: 10.2355/isijinternational.44.115

[35]Rana, R., Bleck, W., Singh, S., & Mohanty, O. (2007). Development of high strength interstitial free steel by copper precipitation hardening. Materials Letters, 61(14-15), 2919–2922. doi: 10.1016/j.matlet.2006.10.037

[36]Gagliano MS. Co-Precipitation of copper and niobium–carbide in a low carbon steel. PhD Thesis, Northwestern University, 2002.

[37]Pavliska J., Jon Z., Mazancová E., Mazanec K., Microstructure and Metallurgy Investigation of the Hot Ductility Behaviour of Steels, Acta Metallurgica Slovaka, (2000) 4, 318–326

[38]Garza-Martinez, L. G. (2003). Workability of 1045 forging steel with residual copper.

[39]S. O'Neill, D. An Investigation of Surface Hot Shortness in Low Carbon Steel, A thesis, School of Materials Science and Engineering, Faculty of Science, The University of New South Wales, Sydney, New South Wales, Australia, March 2002

[40](10th ed.), ASM Metals Hand Book: Properties and Selection: Iron; Steels and High Performance Alloys vol. 1, ASM International, Materials Park, OH 44073 (1995), 389–

[41]Torkar, M. (2010). Effect of Trace and Residual Elements on the Hot Brittleness, Hot Shortness and Properties of 0.15-0.3 % C Al-Killed Steels with a Solidification Microstructure. Materials and Technology,44(6), 327-333. doi: 669.14:620.1/.2

[42]Shibata, K., Seo, S.-J., Kaga, M., Uchino, H., Sasanuma, A., Asakura, K., & Nagasaki, C. (2002). Suppression of Surface Hot Shortness due to Cu in Recycled Steels. Materials Transactions, 43(3), 292–300. doi: 10.2320/matertrans.43.292

[43]Winful, D. A., Cashell, K. A., Afshan, S., Barnes, A. M., & Pargeter, R. J. (2017). Elevated temperature material behaviour of high-strength steel. Proceedings of the Institution of Civil Engineers - Structures and Buildings, 170(11), 777–787. doi: 10.1680/jstbu.16.00213

[44]Podder, Arijit Saha. "Tempering of a mixture of bainite and retained austenite." (2011).